TECH LIBRARY KAFB, NM
0061211

NASA CONTRACTOR REPORT

NASA CR-2483

NASA CR-2

LOAN COPY: RETURN TO
AFWL TECHNICAL LIBRARY
KIRTLAND AFB, N. M.

A TRIANGULAR THIN SHELL FINITE ELEMENT: NONLINEAR ANALYSIS

G. R. Thomas and R. H. Gallagher

Prepared by
CORNELL UNIVERSITY
Ithaca, N. Y. 14850
for Langley Research Center

NATIONAL AERONAUTICS AND SPACE ADMINISTRATION • WASHINGTON, D. C. • JULY 1975

TECH LIBRARY KAFB, NM
0061211

1. Report No.	2. Government Accession No.	3. Recipient's Catalog No.
NASA CR-2483		

4. Title and Subtitle	5. Report Date
A TRIANGULAR THIN SHELL FINITE ELEMENT: NONLINEAR ANALYSIS	July 1975
	6. Performing Organization Code

7. Author(s)	8. Performing Organization Report No.
G. R. Thomas and R. H. Gallagher	
	10. Work Unit No. 134-14-05-01-00
9. Performing Organization Name and Address	11. Contract or Grant No.
Cornell University Ithaca, N. Y. 14850	NGL-33-010-070
	13. Type of Report and Period Covered
12. Sponsoring Agency Name and Address	Contractor Report
National Aeronautics and Space Administration Washington, D. C. 20546	14. Sponsoring Agency Code

15. Supplementary Notes

Topical Report - Companion report to NASA CR-2482

16. Abstract

Aspects of the formulation of a triangular thin shell finite element which pertain to geometrically nonlinear (small strain, finite displacement) behavior are described. The procedure for solution of the resulting nonlinear algebraic equations combines a one-etep incremental (tangent stiffness) approach with one iteration in the Newton-Raphson mode. A method is presented which permits a rational estimation of step size in this procedure. Limit points are calculated by means of a superposition scheme coupled to the incremental side of the solution procedure while bifurcation points are calculated through a process of interpolation of the determinants of the tangent-stiffness matrix. Numerical results are obtained for a flat plate and two curved shell problems and are compared with alternative solutions.

17. Key Words (Suggested by Author(s))	18. Distribution Statement
Finite element Thin shells Displacement approach Nonlinear	Unclassified - Unlimited Subject Category 39

19. Security Classif. (of this report)	20. Security Classif. (of this page)	21. No. of Pages	22. Price*
Unclassified	Unclassified	69	$4.25

*For sale by the National Technical Information Service, Springfield, Virginia 22151

TABLE OF CONTENTS

LIST OF SYMBOLS

A,B	Metric Coefficients of shell surface.
{a}	Vector of generalized displacements.
$[B],[B_{uv}],[B_w]$	Matrices of coefficients in the relationships between strains and joint displacements.
[C]	Coefficient matrix of constraint equations.
[D]	Coefficient matrix of elastic constants.
{d}	Vector of displacement derivatives.
{f}	Vector of out-of-balance forces.
[G]	Transformation of generalized displacements to displacement derivatives.
[H]	Transformation matrix of nonlinear strain displacement equations.
[J]	Transformation matrix of joint to generalized displacements.
$[K_o],[K_1],[K_2]$	Global linear, first- and second-order geometric stiffness matrices.
$[K_T]$	Global tangent stiffness matrix.
$[k_o],[k_1],[k_2]$	Element linear, first- and second-order geometric stiffness matrices
[L]	Row matrix of derivatives of linear strain-displacement equations.
N	Displacement shape functions.
$\bar{P}$	Normalized applied load vector.
R_1,R_2	Radii of curvature of undeformed shell surface in the α and β directions.
T	The twist curvature of the undeformed shell surface.

t	Plate thickness.
u,v,w	Displacement components in α, β and normal directions, respectively.
u , v	Vectors of joint displacements in the in-surface directions.
V	Potential of applied loads.
w	Vector of joint displacements pertinent to radial displacement component.
α,β	Orthogonal curvilinear coordinate system.
α_i,β_i	Nodal coordinate values.
Δ	Nodal displacements.
$\{\varepsilon\}$	Strain vector.
$\varepsilon_1,\varepsilon_2$	Direct strains in the α and β directions respectively.
$\varepsilon_i,\varepsilon_{ij}$	Typical strains.
Φ_1,Φ_2	Rotations of tangent to shell in α and β directions.
ϕ_n^r	Rotation of tangent to the shell which is normal to an edge of element r.
ϕ	Inplane shear strain.
κ_1,κ_2	Strain curvatures in the α and β directions.
η	Load intensity.
$\{\sigma\}$	Stress vector.
τ	Twist strain curvature
Π_p	Potential energy

NOTE: Except for cases given above, or where used to denote differentiation ($u_x = \frac{\partial u}{\partial x}$, $w_{yy} = \frac{\partial^2 w}{\partial y^2}$, etc.) subscripts and superscripts are defined in text where they appear.

LIST OF FIGURES

INTRODUCTION

This report is the second of a pair of reports dealing with the formulative aspects of a capability for finite element thin shell instability analysis. The first report (Ref. 1) was devoted to development of the linear stiffness relationships for a doubly-curved triangular thin shell finite element. The present report describes the extension of these relationships to account for geometrically nonlinear phenomena, which encompass the instability effects of interest to this study, and the procedures used in calculation of a variety of nonlinear solutions and instability load intensities.

A large share of the literature on finite element analysis of the past decade has been devoted to the area of nonlinear analysis. Due to this rapid and continuing rate of progress a number of state-of-the-art surveys have appeared. Martin (Ref. 2) examined this topic in 1969. Subsequently, Oden (Ref. 3) gave an assessment that covered a wider range of nonlinearities. Stricklin and co-workers have presented a number of reviews, one of the more recent being Ref. 4. Gallagher (Ref. 5) also has reviewed the aspects of solution procedures of geometrically nonlinear analysis. Because of this extensive available literature the present report does not attempt a review of the same material, although in the body of the report justification is generally given for the choice of particular procedures in preference to available alternatives.

In addressing problems of geometrically nonlinear analysis a decision must be made relative to the coordinate system

to which all basic relationships are to be referenced. The Lagrangian, or fixed frame of reference is adopted in this report in preference to the Eulerian, or moving, coordinate system. The largest share of work in geometrically nonlinear finite element analysis has adopted the former, although it should be added that selection is most likely one of taste since insufficient evidence has been accumulated of the relative efficiency of these alternatives in the total analysis scheme. Progress in the Eulerian approach is described by Yamada (Ref. 6).

The present work is also restricted to small strain states, so as to preserve the applicability of the linear stress-strain law.

The theoretical basis of the developments described herein is the principle of stationary potential energy. This means that the fundamental relationships consist solely of the stress-strain law and the appropriate strain-displacement relationships. The transformation from continuum form to algebraic relationships is effected on the basis of element assumed displacement fields. This approach, of necessity, follows from the adoption of the same approach in the formulation of the linear stiffness relationships in Ref. 1. It is pertinent to note that alternative variational principles are not well developed in the area of geometrically nonlinear analysis, nor is it apparent that they would possess special advantages in finite element analyses of the subject class of problem.

The finite element formulation described in this report is not in strict adherence to the principle of stationary potential energy because of deficiencies in the satisfaction of conditions on interelement displacement continuity and on zero strain under rigid body motion. It is noted that their severity is reduced to acceptable proportions by means of interelement constraint conditions, and by the choice of the element displacement fields, and also that no new considerations in these respects are introduced by the extension to geometrically nonlinear analysis.

The report is organized as follows. First, reviews are given of the types of geometrically nonlinear behavior likely to be sustained by thin shell structures and of the essential features of the linear stiffness formulation of the shell element treated herein. The latter enables one to read this report without recourse to Ref. 1. The formulation of both the element and global representations for the geometrically nonlinear finite element analysis of thin shells is then established without reference to a specific type of element, after which details are given of the formulation of the subject triangular shell element. The nonlinear formulation is presented in both a rigorous, or "consistent" manner, in which the displacement field employed is that which was used in constructing the linear stiffness terms, and in an approximate manner in which a simple linear displacement field is described over a quadrilateral region consisting of four triangles.

Two approaches to the solution of the global nonlinear algebraic equations, the Newton-Raphson and incremental methods, are discussed in some detail. The approach adopted, known as the modified incremental method, is one which combines one cycle of each of the above approaches within each load step. It is, of course, desirable to maintain control of the error produced in each step. For this purpose the same section of the report introduces a rational approach to error control, based on treatment of the analysis as an initial value problem.

The two types of instability phenomena, limit points and bifurcational buckling, are studied in separate sections of the report. The limit point scheme is based on a superposition procedure applied within an increment of displacement, wherein all behavior is linearized. Bifurcation loads are determined through a Lagrangian interpolation scheme applied to the load versus tangent stiffness determinant solution points. A distinction is made between calculations for linear and nonlinear states preceding bifurcation.

The report concludes with a description of four numerical examples. The postbuckling response of a uniformly compressed flat plate with initial imperfections is studied for a variety of gridworks, solution algorithms, and support conditions. Analyses of a cylindrical shell segment under uniform radial load, a spherical cap under concentrated load at the crown and a clamped square plate under pressure are also described. Comparisons are made in all cases with the results of available alternative numerical or analytical solutions.

2. GEOMETRICALLY NONLINEAR BEHAVIOR OF SHELLS

An understanding of the types of geometrically nonlinear response likely to be sustained by thin shell structures is essential to the construction of basic formulations and algorithms which allow such response to be predicted analytically through the finite element method.

The behavior of all structures at low load levels can be classified in one of three ways (Fig. 1).

i) Linear load-deflection relationship

ii) Nonlinear weakening

iii) Nonlinear stiffening

Common examples of weakening structures are shallow trusses, arches, or shells subjected to inwardly directed loads. The same structures are stiffening if the loads are directed outwards. Examples of both types of structures are shown in Fig. 1.

The work described in this report is mainly concerned with nonlinear weakening situations and to describe in more detail the behavior to be anticipated, Fig. 2 has been drawn. The solid line (OB) applies to "perfect" structures and, for instability problems, represents the case in which the structure first displaces along the OA portion of the path (the fundamental path) and bifurcates (or branches) at the point A. Thus, uniqueness in the definition of the path is lacking at the point A. It should also be noted, in passing, that the assumption is often made in analytical approaches that the fundamental path is linear in the range OA.

The post-buckling path may rise (path AC, Fig. 2a), or it may descend (path AD, Fig. 2b). The slope of the post-buckling path of the perfect structure gives an indication of the behavior to be expected of real structures, which inevitably possess fabricational imperfections. For structures with fabricational imperfections the load-displacement behavior in the presence of destabilizing phenomena follows the paths indicated by dotted lines. In such cases there is no bifurcation phenomenon. Structures with a rising post-buckling path as in Fig. 2a will have strength exceeding the bifurcation load. Imperfect structures with a descending post-buckling path in the perfect state (Fig. 2b) will not achieve strengths as high as the bifurcation load unless the load-displacement path again rises at larger displacements. Such structures, under the appropriate load condition, are therefore imperfection sensitive and the maximum load attained (Point E) is termed the limit point. The instability phenomenon which occurs at this point is known as snap-through, in identification with the physical circumstance of structures in this mode of load-displacement response. A non-bifurcating load-displacement behavior of the limit point (or snap-through) type may also occur for a structure devoid of imperfections. It should be cautioned that the realm of possibilities of structural instability phenomena is not exhausted by the circumstances defined in Fig. 2. Nevertheless, many common structures behave in this manner; some familiar examples are portrayed in Fig. 3.

3. REVIEW OF BASIC ELEMENT REPRESENTATION

A brief review is given in this section of the features of the triangular thin shell element formulation for linear analysis. The review serves to define basic data and theoretical considerations needed for the extension of this formulation to accommodate geometrically nonlinear behavior. The three principal aspects of the linear formulation are (a) the mode of geometric description, (b) the adopted strain-displacement equations, and (c) the selection of displacement functions. Also special considerations arise in the treatment of displacement incompatibilities along the element juncture lines. Each of these items is discussed in the following.

The basic geometry of the triangular shell element is shown in Fig. 4. Points are located on the shell surface in the orthogonal curvilinear system α-β. The user provides nodal values for the three curvatures as well as the shell thickness t. These variables are interpolated linearly over the area of the element.

The strain-displacement equations given by Koiter (Ref. 7) are used in constructing the element potential energy for linear analysts. Koiter's relationships are described as "consistent", i.e., terms of the order of the ratio of the membrane strain to the radius of curvature are retained or discarded in a consistent manner. Also, these relationships evidence no strain under rigid body motion.

In discretizing the potential energy expression formed with use of the strain-displacement equations, the same displacement functions are chosen for u, v and w. Each is in

the form of a complete cubic polynomial, of 10 terms, for which the corresponding displacement fields are

$$u = \lfloor N \rfloor \{u\}, \quad v = \lfloor N \rfloor \{v\}, \quad w = \lfloor N \rfloor \{w\} \tag{1}$$

where $\lfloor N \rfloor = \lfloor N_1 \; N_{\alpha_1} \; N_{\beta_1} \; N_2 \; \ldots \; N_{\beta_3} \; N_4 \rfloor$

$$\{u\} = \lfloor u_1 \; (\frac{\partial u}{\partial \alpha})_1 \; (\frac{\partial u}{\partial \beta})_1 \; u_2 \; \ldots \; (\frac{\partial u}{\partial \beta})_3 \; u_4 \rfloor^T \tag{2}$$

and {v} and {w} are similarly defined. The subscript 4 refers to the centroidal node point. Details of these functions and the reasons for their choice are discussed in Ref. 1. As previously noted, neither of the two factors prominent in the choice of displacement fields for thin shell elements, the condition of zero strain energy under rigid body motion of the element nor that of continuity of angular displacement across element boundaries, are satisfied by the chosen functions, Eq. (1). The use of cubic functions for in-surface displacement components (u and v) represents a move in the direction of the implicit satisfaction of the former condition.

The failure to meet conditions on the interelement continuity of angular displacement has more serious consequences on solution accuracy and for this reason special steps are taken to "restore" this continuity. The approach taken, and indeed the use of a cubic polynomial in representation of the flat triangular element, was introduced by Anderheggen (Ref. 34) and Harvey and Kelsey (Ref. 8). If A and B are neighboring elements and the subscript n denotes the normal

direction, the relative angular displacement of adjacent edges at their midpoint i can be set to zero to ensure inter-element continuity.

$$\left(\frac{\partial w}{\partial \eta}\right)_i = \left(\frac{\partial w}{\partial \eta}\right)_i^A - \left(\frac{\partial w}{\partial \eta}\right)_i^B = 0 \tag{3}$$

Now, the differentiation of the displacement field w yields the angular displacement in terms of the joint displacements, so that a constraint equation of the following form can be written

$$\{C_{A-B}\}^T\{\Delta\} = 0 \tag{4}$$

The above process is applied to each of the m element boundaries and for a system with n degrees-of-freedom the following m by n set of equations is obtained

$$[C]\ \{\Delta\} = 0 \tag{5}$$

Eq. (5) is supplemental to the basic force-displacement relationships of the stiffness analysis. The manner in which such constraint equations are used to modify the basic force-displacement relationships is taken up at the close of the next section.

4. FORMULATION OF NONLINEAR PROBLEM

The derivation given in this section is based on the principle of stationary potential energy. The potential energy (Π_p) of a shell element can be written in the following general form

$$\Pi_p = \frac{1}{2}\int_A \lfloor \varepsilon \rfloor [D]\{\varepsilon\}\, dA + V \tag{6}$$

where A is the surface area of the shell

$\lfloor \varepsilon \rfloor$ is the row vector of relevant strain components ($\{\varepsilon\} = \lfloor \varepsilon \rfloor^T$)

$[D]$ is the matrix of constants in the relationships between the strains and the corresponding stresses, in the form $\{\sigma\} = [D]\ \{\varepsilon\}$.

V is the potential of the applied loads.

For simplicity, a more explicit statement of the potential of the applied loads is deferred until Eq. (6) has been discretized and developed in greater detail.

The present work is concerned with geometric nonlinearities, whose representation is embodied in the strain-displacement equations. Such equations can be expressed in the following general form

$$\{\varepsilon\} = \{\varepsilon^L\} + \{\varepsilon^N\} \tag{7}$$

where $\{\varepsilon^L\}$ gives the linear portion of the strain-displacement equations in terms of displacements and $\{\varepsilon^N\}$ gives the nonlinear portion. The present work adopts a Lagrangian frame of reference for the construction of these relationships, i.e., all quantities are referenced to the axes of the undeformed state. Thus, for the illustrative example of an axial member (Fig. 5)

$$\varepsilon^L = \frac{du}{dx}$$

and

$$\varepsilon^N = \frac{1}{2}\left(\frac{du}{dx}\right)^2 + \frac{1}{2}\left(\frac{dv}{dx}\right)^2 + \frac{1}{2}\left(\frac{dw}{dx}\right)^2$$

The present work also assumes that the direct and shear

strains are small, so that the first term in the expression for ε^N is discarded, as are similar terms in the expressions for $\{\varepsilon^N\}$ for shell behavior.

By substitution of Eq. (7) into Eq. (6) there is obtained

$$\Pi_p = \frac{1}{2}\int_A [\lfloor\varepsilon^L\rfloor [D]\{\varepsilon^L\} + \lfloor\varepsilon^L\rfloor [D]\{\varepsilon^N\} + \lfloor\varepsilon^N\rfloor [D]\{\varepsilon^L\} + \lfloor\varepsilon^N\rfloor [D]\{\varepsilon^N\}]dA + V \tag{7a}$$

This expression will next be discretized with use of the same displacement fields chosen for the linear formulation, Eqs. (1). For conciseness the three components u, v and w are grouped under the symbol $\underline{\Delta}$ and Eq. (1) can be restated as

$$\underline{\Delta} = [N]\{\Delta\} \tag{8}$$

where $\{\Delta\}$ is a 30x1 vector which lists the joint displacements in the order defined below Eq. (1). The 3x30 matrix [N] is similarly arrayed. By performance of the operations dictated by the strain-displacement relationships the discretized form of the strains is given by

$$\{\varepsilon^L\} = [B^L]\{\Delta\} \tag{9a}$$

$$\{\varepsilon^N\} = [B^N]\{\Delta\} \tag{9b}$$

The terms of $[B^L]$ are constants and functions of the surface coordinates and the terms of $[B^N]$ are functions of the displacements $\{\Delta\}$ as well as of constants and the surface coordinates.

After substitution of Eqs. (9a) and (9b) into Eq. (7a) and performance of the indicated integration the finite element (discretized) potential energy $\underset{\sim}{\Pi}_p$ is obtained. In indicial notation

$$\underset{\sim}{\Pi}_p = \frac{1}{2} \underset{\sim}{k_o}_{ij} \underset{\sim}{\Delta}_i \underset{\sim}{\Delta}_j + \frac{1}{6} k_{1_{ijk}} \underset{\sim}{\Delta}_i \underset{\sim}{\Delta}_j \underset{\sim}{\Delta}_k + \frac{1}{12} k_{2_{ijk\ell}} \underset{\sim}{\Delta}_i \underset{\sim}{\Delta}_j \underset{\sim}{\Delta}_k \underset{\sim}{\Delta}_\ell + \underset{\sim}{V} \qquad (10a)$$

in which $k_{o_{ij}}$, $k_{1_{ijk}}$, and $k_{2_{ijk\ell}}$ are second, third and fourth order tensors and are fixed values for a given element, and V is the potential of any applied loads on the surface of the element. The subscript tilde (~) denotes that these are element quantities. Alternatively, in matrix notation

$$\underset{\sim}{\Pi}_p = \frac{\lfloor \underset{\sim}{\Delta} \rfloor}{2} [\underset{\sim}{k_o}] \{\underset{\sim}{\Delta}\} + \frac{1}{6} \lfloor \underset{\sim}{\Delta} \rfloor [\underset{\sim}{k_1}(\Delta)] \{\underset{\sim}{\Delta}\} + \frac{1}{12} \lfloor \underset{\sim}{\Delta} \rfloor [\underset{\sim}{k_2}(\Delta^2)] \{\underset{\sim}{\Delta}\} + \underset{\sim}{V} \qquad (10b)$$

The matrices $[k_o]$, $[k_1(\Delta)]$ and $[k_2(\Delta^2)]$ are the linear and first-order and second order geometric element stiffness matrices, respectively. The symbols (Δ) and (Δ^2) are inserted adjacent to k_1 and k_2 to emphasize that terms of these matrices are, respectively, linear and quadratic functions of the displacements $\{\Delta\}$. Elsewhere in this report, with certain exceptions, these matrices will simply be denoted as $[k_1]$ and $[k_2]$. It is also noted that other reports of this research (Refs. 9 and 10) have designated these matrices as $[n_1]$ and $[n_2]$. To avoid confusion with the designation of shape functions given in this and the companion report, however, these matrices are designated as $[k_1]$ and $[k_2]$ herein.

For simplicity consideration is given only to concentrated applied loads P_i acting at the degrees-of-freedom Δ_i. Also, for the conditions of the present work it is assumed that a fixed distribution of normalized loads $\overline{P}_i$ prevails at all intensities of load η so that the loads are alternatively written as $P_i = \eta\, \overline{P}_i$. The potential of the applied loads is therefore $V = \lambda\, \overline{P}_i\, \Delta_i$, where the summation convention of indicial notation prevails. The potential energy of the complete structure is evaluated by summing the contributions of all elements and of V. In indicial notation

$$\Pi_p = \frac{1}{2} K_{o_{ij}} \Delta_i \Delta_j + \frac{1}{6} K_{1_{ijk}} \Delta_i \Delta_j \Delta_k + \frac{1}{12} K_{2_{ijk\ell}} \Delta_i \Delta_j \Delta_k \Delta_\ell - \eta\, \overline{P}_i \Delta_i \tag{11a}$$

Alternatively, in matrix notation

$$\Pi_p = \frac{1}{2} \lfloor \Delta \rfloor\, [K_o]\{\Delta\} + \frac{1}{6} \lfloor \Delta \rfloor\, [K_1(\Delta)]\{\Delta\} + \frac{1}{12} \lfloor \Delta \rfloor\, [K_2(\Delta^2)]\{\Delta\} - \eta \lfloor \Delta \rfloor \{\overline{P}\} \tag{11b}$$

The matrices $[K_o]$, $[K_1(\Delta)]$ and $[K_2(\Delta^2)]$ are the global linear and first and second order geometric stiffness matrices and again the dependence of the latter two on $\{\Delta\}$ has been emphasized.

By taking the first variation of Π_p with respect to each degree-of-freedom (Δ_i) in turn, and setting each to zero in accordance with the stationary property of potential energy, and noting that the first three terms on the right side are quadratic, cubic, and quartic functions, respectively, of the degrees of freedom, one obtains the nonlinear algebraic equations of equilibrium. In indicial notation

$$K_{o_{ij}}\Delta_j + \frac{1}{2} K_{1_{ijk}}\Delta_j\Delta_k + \frac{1}{3} K_{2_{ijk\ell}}\Delta_j\Delta_k\Delta_\ell - \eta \bar{P}_i = 0 \qquad (12a)$$

or, in matrix notation

$$[K_o]\{\Delta\} + \frac{1}{2}[K_1]\{\Delta\} + \frac{1}{3}[K_2]\{\Delta\} - \eta\{\bar{P}\} = 0 \qquad (12b)$$

It is to be observed that special care must be taken in the construction of the $[K_1]$ and $[K_2]$ matrices so that the simple mode of differentiation indicated above (e.g. $\frac{d}{d\{\Delta\}}(\frac{\lfloor\Delta\rfloor}{6}[K_1]\{\Delta\}) = \frac{1}{2}[K_1]\{\Delta\}$) holds true. This point is elaborated upon in the next section.

No explicit consideration has been given in the foregoing to the constraint conditions (Eq. (5)) which are necessary for the restoration of interelement displacement continuity. The next section will show that these constraints do not influence the nonlinear matrices $[K_1]$ and $[K_2]$. Thus, only $[K_o]$ is influenced and it is assumed that the full linear portion of the equilibrium equations are in fact of the form

$$\begin{bmatrix} K_o & C^T \\ C & 0 \end{bmatrix}$$

5. FORMULATION OF ELEMENT NONLINEAR MATRICES

a. Consistent-Triangle

This section is devoted to a detailed description of the formulation of the nonlinear matrices $[K_1]$ and $[K_2]$, which were introduced in the previous section, for the specific case of the subject triangular thin shell element. A cor-

respondingly detailed description of the formulation of the linear stiffness matrix $[k_o]$ is given in Ref. 1. The present formulation adheres to the notion of "consistency", wherein the displacement functions employed in the construction of $[k_1]$ and $[k_2]$ are identically those employed for $[k_o]$. This results in a high cost of formulation for $[k_1]$ and $[k_2]$, so in the latter portion of this section a more economical, inconsistent, formulation is described.

To establish the desired formulations, it is appropriate to compare terms in Eqs. (7a) and (10b). On this basis it is found that (the tilde underline is neglected, since this clearly refers to the individual element)

$$\frac{1}{6}\lfloor\Delta\rfloor[k_1]\{\Delta\} = \int_A (\lfloor\varepsilon^N\rfloor[D]\{\varepsilon^L\} + \lfloor\varepsilon^L\rfloor[D]\{\varepsilon^N\})dA \qquad (13)$$

and

$$\frac{1}{12}\lfloor\Delta\rfloor[k_2]\{\Delta\} = \int_A \lfloor\varepsilon^N\rfloor[D]\{\varepsilon^N\}dA \qquad (14)$$

In order to proceed further the specific form of the relevant strain-displacement equations is needed. As noted in Section 2 the adopted linear components of these relationships are those due to Koiter (Ref. 7). The corresponding nonlinear terms have been derived by Mushtari (Ref. 11). The strain components of thin shell behavior are the direct strains of membrane action ε_1 ε_2 and ϕ and for flexure they are the curvatures k_1, k_2 and τ. Mushtari has pointed out that the neglect of nonlinear terms in the curvature expressions is justified in problems of "medium" bending, i.e.,

where the normal displacements are of the same order of magnitude as the thickness of the shell but much smaller than the other dimensions. Adopting this assumption, only the membrane strain-displacement equations are influenced. Hence

$$\varepsilon_1 = \frac{1}{A}\frac{\partial u}{\partial \alpha} + \frac{v}{AB}\frac{\partial A}{\partial \beta} - \frac{w}{R_1} + \underline{\frac{1}{2A^2}\left(\frac{\partial w}{\partial \alpha}\right)^2}$$

$$\varepsilon_2 = \frac{1}{B}\frac{\partial v}{\partial \beta} + \frac{u}{AB}\frac{\partial B}{\partial \alpha} - \frac{w}{R_2} + \underline{\frac{1}{2B^2}\left(\frac{\partial w}{\partial \beta}\right)^2} \qquad (15)$$

$$\phi = \frac{1}{A}\frac{\partial v}{\partial \alpha} + \frac{1}{B}\frac{\partial u}{\partial \beta} - \frac{u}{AB}\frac{\partial B}{\partial \alpha} - \frac{v}{AB}\frac{\partial B}{\partial \alpha} - \frac{2w}{T} + \underline{\frac{1}{2AB}\left(\frac{\partial w}{\partial \alpha}\right)\left(\frac{\partial w}{\partial \beta}\right)}$$

The nonlinear terms are underlined for clarity. A and B are the metric coefficients of the shell surface and R_1, R_2 and T are the radii of curvature of the undeformed shell in the α and β directions.

In view of Eqs. (15), we have

$$\varepsilon_1^L = \frac{1}{A}\frac{\partial u}{\partial \alpha} + \frac{v}{AB}\frac{\partial A}{\partial \beta} - \frac{w}{R_1}$$

$$\varepsilon_1^N = \frac{1}{2A^2}\left(\frac{\partial w}{\partial \alpha}\right)^2$$

$$\varepsilon_2^L = \frac{1}{B}\frac{\partial v}{\partial \beta} + \frac{u}{AB}\frac{\partial B}{\partial \alpha} - \frac{w}{R_2} \qquad (16)$$

$$\varepsilon_2^N = \frac{1}{2B^2}\left(\frac{\partial w}{\partial \beta}\right)^2$$

$$\phi^L = \frac{1}{A}\frac{\partial v}{\partial \alpha} + \frac{1}{B}\frac{\partial u}{\partial \beta} - \frac{u}{AB}\frac{\partial B}{\partial \alpha} - \frac{v}{AB}\frac{\partial B}{\partial \alpha} - \frac{2w}{T}$$

$$\phi^N = \frac{1}{2AB}\left(\frac{\partial w}{\partial \alpha}\right)\left(\frac{\partial w}{\partial \beta}\right)$$

By substitution of the shape functions (Eq. (1)) into the above, expressions of the following form are obtained (consistent with the symbolism of Eqs. (9a) and (9b))

$$\varepsilon_1^L = \lfloor B_{uv}^L \; B_w^L \rfloor \begin{Bmatrix} u \\ v \\ -- \\ w \end{Bmatrix} \tag{17}$$

$$\varepsilon_1^N = \frac{1}{2} \lfloor 0 \quad B_w^N \rfloor \begin{Bmatrix} u \\ v \\ -- \\ w \end{Bmatrix} \lfloor 0 \quad B_w^N \rfloor \begin{Bmatrix} u \\ v \\ -- \\ w \end{Bmatrix} \tag{18}$$

and similar expressions for ε_2^L, ε_2^N, ϕ^L and ϕ^N.
When expressions (17) and (18) are substituted in Eq. (13) terms of the following form are encountered.

$$\int_A \lfloor B_{uv_i}^L \; B_{w_i}^L \rfloor \begin{Bmatrix} u \\ v \\ -- \\ w \end{Bmatrix} \lfloor 0 \quad B_w^N \rfloor \begin{Bmatrix} u \\ v \\ -- \\ w \end{Bmatrix} \lfloor 0 \quad B_w^N \rfloor \begin{Bmatrix} u \\ v \\ -- \\ w \end{Bmatrix} dA \tag{19}$$

The summation of these terms can be designated in indicial form as $k_{1_{ijk}} \Delta_i \Delta_j \Delta_k$. The calculation of $k_{1_{ijk}}$, once and for all, would seem to be an attractive approach. Unfortunately, excessive computer storage required for the tensor prohibits this. Because of this the structure of Eq. (19) is reduced to quadratic form so that the kernel $[k_1]$ is a function of the displacements. This is done in the following manner.

$$\varepsilon_i^L \; \varepsilon_j^N \varepsilon_k^L = \frac{1}{6} [\varepsilon_i^L (\varepsilon_j^N)^T \varepsilon_k^N + \varepsilon_i^L \; (\varepsilon_k^N)^T \varepsilon_j^N + \varepsilon_j^N \; (\varepsilon_k^N)^T \varepsilon_i^L + \varepsilon_j^N (\varepsilon_k^N)^T \varepsilon_i^L$$

$$\varepsilon_k^N \; (\varepsilon_i^L)^T \varepsilon_j^N + \varepsilon_k^N \; (\varepsilon_j^N)^T \varepsilon_i^L] \tag{20}$$

Typically, by invoking the nomenclature of Eqs. (17) and (18), the first term on the right side of Eq. (20) can be written as

$$\frac{1}{6}\left[\left[B^L_{uv_i}\,\middle|\,B^L_{w_i}\right]\begin{Bmatrix}u\\v\\-\\w\end{Bmatrix}\begin{bmatrix}u & v & | & w\end{bmatrix}\begin{Bmatrix}0\\B^N_{w_j}\end{Bmatrix}\left[0\,\middle|\,B^N_{w_k}\right]\begin{Bmatrix}u\\v\\--\\w\end{Bmatrix}\right]$$

$$= \frac{1}{6}\left(\left[B^L_{uv_i}\right]\begin{Bmatrix}u\\v\end{Bmatrix} + \left[B^L_{w_i}\right]\{w\}\right)\begin{bmatrix}u & v & | & w\end{bmatrix}\left[\begin{array}{c|cc}0 & 0 & 0\\ \hline 0 & B^N_{w_j} & B^N_{w_k}\end{array}\right]\begin{Bmatrix}u\\v\\-\\w\end{Bmatrix} \tag{21}$$

which is the desired quadratic form. This procedure of transforming the product of three strain quantities into quadratic form with a nonlinear kernel is applied in the same manner to develop all terms of $[k_1]$. A listing of all of the resulting terms can be found in Ref. 12. Clearly, the integration of these terms cannot be performed explicitly, so that a numerical integration, must be adopted. A 4 x 4 Gaussian scheme is employed, as in the case of $[k_o]$ in Ref. 1.

The number of matrix operations required can be reduced considerably in two ways. First, by taking advantage of symmetry, and secondly by noting that many of the matrices present can be obtained by transposing others.

The same approach as that delineated above is used in calculating $[k_2]$. In this case products of four strains are converted to a quadratic form. The basic components of the $[k_2]$ matrix have the following structure

$$\int_A \begin{bmatrix} 0 & B^N_{w_i} \end{bmatrix} \begin{Bmatrix} u \\ v \\ -- \\ w \end{Bmatrix} \begin{bmatrix} 0 & B^N_{w_i} \end{bmatrix} \begin{Bmatrix} u \\ v \\ -- \\ w \end{Bmatrix} \begin{bmatrix} 0 & B^N_{w_j} \end{bmatrix} \begin{Bmatrix} u \\ v \\ -- \\ w \end{Bmatrix} \begin{bmatrix} 0 & B^N_{w_j} \end{bmatrix} \begin{Bmatrix} u \\ v \\ -- \\ w \end{Bmatrix} dA$$

In indicial notation this would be $k_{2_{ijk\ell}} \Delta_i \Delta_j \Delta_k \Delta_\ell$. The equation corresponding to Eq. (20) for four strains is

$$\begin{aligned} \varepsilon^N_i \varepsilon^N_i \varepsilon^N_j \varepsilon^N_j = \frac{1}{6} \, & (\varepsilon^N_i \varepsilon^N_i (\varepsilon^N_j)^T \varepsilon^N_j + \varepsilon^N_i \varepsilon^N_j (\varepsilon^N_i)^T \varepsilon^N_j + \varepsilon^N_i \varepsilon^N_j (\varepsilon^N_j)^T \varepsilon^N_i \\ & + \varepsilon^N_j \varepsilon^N_j (\varepsilon^N_i)^T \varepsilon^N_i + \varepsilon^N_j \varepsilon^N_i (\varepsilon^N_j)^T \varepsilon^N_i + \varepsilon^N_j \varepsilon^N_i (\varepsilon^N_i)^T \varepsilon^N_j) \end{aligned} \tag{23}$$

The first term on the right side is rewritten as

$$\frac{1}{6} \begin{bmatrix} 0 & 1 & B^N_{w_i} \end{bmatrix} \begin{Bmatrix} u \\ v \\ -- \\ w \end{Bmatrix} \begin{bmatrix} 0 & B^N_{w_i} \end{bmatrix} \begin{Bmatrix} u \\ v \\ -- \\ w \end{Bmatrix} \begin{bmatrix} u & v & w \end{bmatrix} \begin{Bmatrix} 0 \\ -- \\ (B^N_{w_j})^T \end{Bmatrix} \begin{bmatrix} 0 & B^N_{w_j} \end{bmatrix} \begin{Bmatrix} u \\ v \\ -- \\ w \end{Bmatrix}$$

$$= \frac{1}{6} (B^N_{w_i} w)^2 \begin{bmatrix} u & v & w \end{bmatrix} \left[\begin{array}{c|c|c} 0 & -- & \frac{0}{T} \\ \hline 0 & (B^N_{w_j}) & B^N_{w_j} \end{array}\right] \begin{Bmatrix} u \\ v \\ -- \\ w \end{Bmatrix} \tag{24}$$

which again is the desired form. By substituting terms of this sort for each product of two nonlinear strains in the energy relationship (Eq. (14)), the $[k_2]$ matrix is obtained. Details of the resulting matrix are presented in Ref. 12.

It is recalled (see Ref. 1 and Sect. 4 of this report) that the linear stiffness matrix that is relevant to the present study contains three rows and columns that correspond to constraint equations to enforce interelement continuity.

The coefficients in these equations are constants that depend only on the element shape. Since the inplane displacements are considered to be negligible, the change in element shape is discounted. Consequently the constraint equations need no modification during a nonlinear analysis.

b. Inconsistent - Quadrilateral

Considerable savings in data preparation and computer execution times can be realized by the use of quadrilateral elements as compared to triangular elements. In the present work four triangles are combined to form a quadrilateral (Fig. 6). Constant curvature is assumed for the new element. Internal degrees of freedom are eliminated from the linear stiffness matrix by the use of static condensation. For nonlinear analysis the geometric stiffness matrices are computed directly for a quadrilateral without consideration of the component triangles as delineated in this section.

The finite element method, when based in variational principles, requires interelement continuity of derivatives up to one order lower than appears in the associated functional, or energy. For the case of plate bending or shell structures continuity of slopes is required of the displacement fields. This conclusion is valid for linear terms. With reference to the strain displacement relationships the highest derivative to appear in the nonlinear terms is the first. Thus, only continuity of the displacements themselves is demanded by the variational principle. This opens up the possibility of using a simplified field for the nonlinear terms as compared to the complex field used for linear terms.

This is the approach adopted herein for the quadrilateral element.

The approach introduced by Mallet and Marcal (Ref. 14) is modified to accommodate the curvature of an element. The strain displacement relationships of Eq. (15) are simplified to read

$$\varepsilon_1 = \frac{\partial u}{\partial \alpha} + \frac{w}{R_1} + \frac{1}{2}\left(\frac{\partial w}{\partial \alpha}\right)^2$$

$$\varepsilon_2 = \frac{\partial v}{\partial \beta} + \frac{w}{R_2} + \frac{1}{2}\left(\frac{\partial w}{\partial \beta}\right)^2 \qquad (15a)$$

$$\phi = \frac{\partial u}{\partial \beta} + \frac{\partial v}{\partial \alpha} + \frac{w}{T} + \left(\frac{\partial w}{\partial \alpha}\right)\left(\frac{\partial w}{\partial \beta}\right)$$

These can be written concisely as (Ref. 13) (with $\phi = \varepsilon_3$)

$$\varepsilon_i = \lfloor L_i \rfloor \{d\} + \frac{1}{2} \lfloor d \rfloor [H_i] \{d\} \qquad (15b)$$

where

$$\lfloor d \rfloor = \left\lfloor \frac{\partial u}{\partial \alpha} \frac{\partial u}{\partial \beta} \frac{\partial v}{\partial \alpha} \frac{\partial v}{\partial \beta} w \frac{\partial w}{\partial \alpha} \frac{\partial w}{\partial \beta} \right\rfloor$$

$$\lfloor L_1 \rfloor = \left\lfloor 1\ 0\ 0\ 0\ \frac{1}{R_1}\ 0\ 0 \right\rfloor$$

$$\lfloor L_2 \rfloor = \left\lfloor 0\ 0\ 0\ 1\ \frac{1}{R_2}\ 0\ 0 \right\rfloor$$

$$\lfloor L_3 \rfloor = \left\lfloor 0\ 1\ 1\ 0\ \frac{1}{T}\ 0\ 0 \right\rfloor$$

$$[H_1] = \begin{bmatrix} 0 & 0 & 0 & 0 & 0 & 1 & 0 \end{bmatrix}$$

$$[H_2] = \begin{bmatrix} 0 & 0 & 0 & 0 & 0 & 0 & 1 \end{bmatrix}$$

$H_3(i,j) = 0$, except for $H_3(6,7) = H_3(7,6) = 1$

By introducing Eq. (15a) into the energy expressions, Eqs. (13) and (14), "core" forms of the first-and second-order geometric stiffness matrices can be established. These are denoted by $[\hat{k}_1]$ and $[\hat{k}_2]$ and are given by

$$[\hat{k}_1] = \int_A t\, C_{ij} \left(\{L_i\} \lfloor d \rfloor [H_j] + \lfloor d \rfloor \{L_i\}[H_j] + [H_i]\{d\}\lfloor L_j \rfloor\right) dA \qquad (25a)$$

$$[\hat{k}_2] = \int_A t\, C_{ij} \left([H_i]\{d\} \lfloor d \rfloor [H_j] + \frac{1}{2} \lfloor d \rfloor [H_j]\{d\}[H_i]\right) dA \qquad (25b)$$

where C_{ij} is the material compliance and t is the thickness of the shell. These matrices, which are independent of the displacement field postulated for the element, are detailed in Ref. 12.

In the present development a bilinear assumption is made for each of the three components of displacement, i.e.

$$\begin{aligned} u &= a_1 + a_2\alpha + a_3\beta + a_4\alpha\beta \\ v &= a_5 + a_6\alpha + a_7\beta + a_8\alpha\beta \\ w &= a_9 + a_{10}\alpha + a_{11}\beta + a_{12}\alpha\beta \end{aligned} \qquad (26)$$

By appropriate differentiation, vector {d} can be expressed in terms of the coefficients {a}. Thus

$$\{d\} = [G]\{a\} \qquad (27)$$

It is also necessary to express the generalized coefficients {a} in terms of the nodal displacements {Δ}. This is done by evaluating the polynomials of Eq. (26) at the node points.

$$\{a\} = [J]\{\Delta\} \tag{28}$$

The ingredients for forming the geometric stiffness matrices with respect to the nodal displacements are now ready. Thus

$$[k_1] = [J]^T \int_A [G]^T [\hat{k}_1][G]dA\ [J]$$

$$= [J]^T [\tilde{k}_1][J] \tag{29a}$$

and

$$[k_2] = [J]^T[\tilde{k}_2][J] \tag{29b}$$

The necessary integration operations for $[\tilde{k}_1]$ and $[\tilde{k}_2]$ can be performed explicitly. This has been done in the present case, with results given in detail in Ref. 12. Because of this ability for calculation of explicit terms the calculation of the inconsistent matrices for the quadrilateral is far more rapid than the consistent formulation calculation for the triangle.

6. SOLUTION OF NONLINEAR EQUATIONS

a. Newton-Raphson Method

As noted in the Introduction, algorithms for the solution of the nonlinear algebraic equations representing geometrically nonlinear behavior (e.g., Eq. (12b)) have attracted a great deal of attention from researchers. No one algorithm has gained universal preference over the others, mainly because each method is effective for particular situations but inefficient or invalid for different situations. The approach adopted in the present work is therefore a combination of two

basic schemes, the Newton-Raphson and incremental methods respectively, and each of these is outlined in the present section. Another view of pertinent algorithms is that the analysis can be treated as an initial value problem. This view gives a different perspective on the methods adopted and also is a basis of a procedure for rational selection of load increment selection. Hence, the initial value analysis concept is also discussed herein. A concluding portion of the section ties together the overall strategy for solution of the pertinent nonlinear equations.

To describe the Newton-Raphson approach it is convenient to rearrange Eq. (12b) as follows

$$\{f\} = [k_o]\{\Delta\} + \frac{1}{2}[k_1]\{\Delta\} + \frac{1}{3}[k_2]\{\Delta\} - \eta\{\bar{P}\} = 0 \qquad (30)$$

where $\{f\}$ is an imbalance of load. A nonlinear analysis must proceed on the basis of an estimate of $\{\Delta\}$ and improve on the estimate in succeeding iterations. By expanding in a Taylor series about an approximate $\{f_i\}$, after i iterations

$$\{f_{i+1}\} = \{f_i\} + \left[\frac{\partial\{f_i\}}{\partial\Delta}\right]\{d\Delta\} + \text{higher-order terms in } \{d\Delta\} \qquad (31)$$

where $\{d\Delta\} = \{\Delta_{i+1}\} - \{\Delta_i\}$ is the change of displacements. With neglect of higher-order terms and with $\{f_{i+1}\}$ set equal to zero, we have

$$\{\Delta_{i+1}\} = \{\Delta_i\} - \left[\frac{\partial\{f_i\}}{\partial\Delta}\right]^{-1}\{f_i\} \qquad (32a)$$

or using the nomenclature of equation 30

$$\{\Delta_{i+1}\} = \{\Delta_i\} - [K_o+K_1+K_2]^{-1}\{f_i\} \qquad (32b)$$

The iteration continues until $\{\Delta_{i+1}\}$ is arbitrarily close to $\{\Delta_i\}$.

It is apparent that the "inversion" of a large matrix is called for at each iteration. To circumvent this problem the matrix of stiffness coefficients can be held fixed for several iterations so that modifications only to the residual load vector {f} are required. This approach is usually called the modified Newton-Raphson method. Its relationship to the standard Newton-Raphson method for a one-degree-of-freedom problem is shown graphically in Figure 7.

It is obvious from Figure 7 that the convergence characteristics of the modified approach are inferior to the standard method but, because each iteration is cheaper in computational effort, the overall cost could well be less. Two factors have a bearing on this outcome. First is the number of equations in the system. For a large order system the expense of repeated 'inversion' becomes very high. On the other hand, because of the increased number of iterations for the modified approach, the geometric stiffness matrices have to be evaluated a greater number of times. For simple (usually inconsistent) formulations these element form times are insignificant, but for complex derivations the times can compound to be greater than the time needed for solving the linear equations at each iteration. It would therefore seem that the standard Newton-Raphson method should be used for an idealization using complex elements where there is a corresponding reduction in the number of freedoms. The modified approach would be more competitive for large problems using simple elements.

The main disadvantage of the Newton-Raphson method is that it cannot be used in problems for which the solution is path dependent such as plasticity. In that particular instance, elastic unloading could occur during the iterative process which was not experienced by the actual structure. Thus, this method is not suitable for a general purpose program that accommodates geometric and material nonlinearities. Another shortcoming of the method in the form described above is that it does not converge at points of instability. This is so because the tangential stiffness matrix is singular at such points. Thurston (Ref. 15) resolves this difficulty by use of higher order terms in the Taylor series expansion upon which the method is based (Eq. 31). A more popular approach in finite element analysis has been to prescribe displacement increments, rather than load increments, at or near critical points. A form of this approach has been adopted in the present work and is described in Section 7.

Although in theory it is possible to solve the nonlinear system at any load level without previous information, care should be taken in selecting a starting point for the iterative process. Divergence is possible if the starting point is not sufficiently close to the solution. To overcome this problem it is recommended that solutions be achieved at lower load levels so that a reliable starting value can be safely extrapolated.

b. Incremental Method

In this method a solution $\{\Delta + d\Delta\}$ is sought for Eq. (12b)

close to a known solution $\{\Delta\}$. Using a Taylor series expansion for $[K_1]$ and $[K_2]$ we get

$$[K_1(\Delta+d\Delta)]\{\Delta+d\Delta\} = [[K_1(\Delta)] + \frac{d}{d\Delta}[K_1(\Delta)]\{d\Delta\} + \ldots]\{\Delta+d\Delta\}$$

$$= [[K_1(\Delta)]\{\Delta\} + 2\,[K_1(\Delta)]\{d\Delta\} + \ldots. \qquad (33)$$

and

$$[K_2(\Delta+d\Delta)^2]\{\Delta+d\Delta\} = [K_2(\Delta^2)]\{\Delta\} + 3\,[K_2(\Delta)^2]\{d\Delta\} + \ldots \qquad (34)$$

Neglecting terms of higher order than those shown explicitly on the right hand side, substituting these expressions into Eq. (12b), and collecting terms

$$[[K_o]+[K_1]+[K_2]]\{d\Delta\} = (\eta+d\eta)\{\bar{P}\} - [K_o]\{\Delta\}$$

$$-\frac{1}{2}[K_1]\{\Delta\} - \frac{1}{3}[K_2]\{\Delta\} = d\eta\{\bar{P}\} + \{f\} \qquad (35)$$

By assuming that equilibrium is satisfied exactly at a load level denoted by η this equation can be simplified by substituting $\{f\} = 0$

$$[[K_o] + [K_1] + [K_2]]\{d\Delta\} = d\eta\,\{\bar{P}\}$$

or

$$[K_T]\,\{d\Delta\} = d\eta\,\{\bar{P}\} \qquad (36)$$

This is the basic equation of the incremental method. Thus at each load level one 'inversion' of the stiffness matrix is required, but the displacements are directly available without any iteration. This approach is ideally suited for tracing the load-deflection behavior of a structure,

especially in the presence of material nonlinearities where small load increments are required to follow the spread of plastic zones.

The main inaccuracy inherent in the incremental method is the gradual divergence from the true solution caused by the piecewise linearizations of a curve. This is shown graphically in Figure 8. This error can be reduced, but not eliminated completely, by using smaller load steps. Another effective device for keeping the divergence to a minimum is to add the out of balance force vector $\{f\}$ of the previous load level to the right hand side at the present load level. When this operation is performed on Eq. (36) one arrives back at Eq. (35). The algorithm indicated by Eq. (35) is called the modified incremental method.

Under close scrutiny it is apparent that Eq. (35) and Eq. (32b) of the Newton-Raphson method are almost identical. The only difference being that in the incremental method $\{d\Delta\}$ is solved directly without iteration. For this reason the modified incremental approach can be thought of as one cycle of the Newton-Raphson procedure.

c. Initial Value Approach for Error Estimate

The geometrically nonlinear problem can be formulated as an initial value problem. When this is done it is possible to identify a variety of established solution techniques which can be applied to the conditions under study. Although these alternatives are not adopted herein it is useful to examine the basic statement of the initial value format. This format sheds some light on the methods outlined

above. Also, it furnishes the basis for a rational scheme of increment step selection.

Eq. (36) can be written in the limit, as $d\eta$ goes to zero, as

$$[[K_o] + [K_1] + [K_2]]\{\Delta\} = \{\dot{P}\} \tag{37}$$

where the dot indicates differentiation with respect to the load level η. The simplest method of solving this equation is Euler's one step method. This yields Eq. (36) of the incremental method, as is to be expected since Euler's formula and Eq. (36) are both derived by expanding about a known solution point by a Taylor series expansion, quadratic and higher terms being discarded.

An algorithm can be derived from Eq. (37) which possesses an accurate estimate of the discretization error. Conversely, with a pre-defined level of acceptable discretization error this algorithm permits the selection of the load increment such that this level will not be exceeded. Thus, the incremental analysis proceeds with variable steps throughout the load-displacement history.

The algorithm in question is based on a method of solution of first-order differential equations attributed to Bulirsh and Stoer (Refs. 16,17). Two separate estimates of displacements are given at every other load increment. These values are averaged before the algorithm is repeated with a new starting point. The basic steps in the method are listed below and shown in Figure 9.

$$
\begin{aligned}
&(1) \quad \{\Delta_{i+1}\} = \{\Delta_i\} + d\eta\, [K_T(\Delta_i)]^{-1}\, \{\bar{P}\} \\
&(2) \quad \{\Delta^A_{i+2}\} = \{\Delta_i\} + 2d\eta\, [K_T(\Delta_{i+1})]^{-1}\, \{\bar{P}\} \\
&(3) \quad \{\Delta^B_{i+2}\} = \{\Delta_{i+1}\} + d\eta\, [K_T(\Delta_{i+2})]^{-1}\, \{\bar{P}\} \\
&(4) \quad \{\Delta_{i+2}\} = \tfrac{1}{2}\, \{\Delta^A_{i+2}\} + \tfrac{1}{2}\, \{\Delta^B_{i+2}\}
\end{aligned}
\tag{38}
$$

To estimate the discretization error of the above procedure, a simple cubic function is used as a test case. Consider the differential equation

$$y' = a + 2bx + 3cx^2$$

which has the obvious solution

$$y = ax + bx^2 + cx^3$$

when $y(0) = 0$

Applying steps (1) thru (4) when the step size is h,

$$y_1 = ah$$

$$y_2^A = 2ah + 4bh^2 + 6ch^3$$

$$y_2^B = ah + (ah + 4bh^2 + 12ch^3)$$

$$y_2 = 2ah + 4bh^2 + 9ch^3$$

$$\delta = y_2^B - y_2^A = 6ch^3$$

But $y(2h)_{exact} = 2ah + 4bh^2 + 8ch^3$

The error, $\varepsilon = ch^3 = 0(h^3)$

or expressed in terms of the difference, δ between the two estimates of y_2,

$$\varepsilon = \frac{\delta}{6}$$

Extending this finding to the multidegree of freedom system, The error is defined as

$$\varepsilon = \frac{1}{6} \text{ Max } \frac{\Delta^A_{i+2,j} - \Delta^B_{i+2,j}}{\Delta_{i+2,j}} \tag{39}$$

where j denotes the freedom number.

The fact that the local discretization error ε is $0(d\eta^3)$ combined with Eq. (39) can be used to either increase or decrease the load step size. Assuming that the predefined error tolerance is denoted by TOL, then if

$$\varepsilon > \text{TOL}$$

The step size is halved, and the procedure initiated from $\{\Delta_i\}$ again. If

$$8\varepsilon < \text{TOL}$$

the step size is doubled.

A simple geometrically nonlinear problem has been solved by the procedure indicated. The test case (Fig. 10) is a shallow truss for which there is an analytical solution as well as other numerical solutions (Ref. 18). For comparison purposes the results from the modified incremental scheme are also displayed in Figure 10. The number of times the stiffness matrix had to be inverted is approximately the same for both methods, and thus the cost of the solutions are comparable. The value of TOL was set at 0.1 for this example. The points A-D illustrate how this tolerance was applied. When the load level reached point A the two subsequent increments produced the values indicated by points B and C. Since these failed to meet the error tolerance they were discarded, the increment

size was halved, and the satisfactory point D was obtained in the succeeding calculation. Although the present approach does not stay as close to the correct solution as the incremental method for most of the path, neither does it drift as far away at certain points.

d. Overall Strategy

In the present study the approach used for nonlinear analysis is the Newton-Raphson method. This method accommodates the modified incremental approach simply by prescribing a very large convergence tolerance factor. By this artifice only one iteration is performed at each load level. It is noted in Section 6b above that the modified incremental method is equivalent to one iteration of the Newton-Raphson method.

Although no results for shell problems can be quoted for the initial value approach mentioned in the last section it is felt that this method holds great promise. This is particularly true for problems for which there are sudden changes in stiffness of the structure (e.g. an imperfect cylinder). It is hoped that this approach can be included in the same computer program as the Newton-Raphson method. This would facilitate the choosing of an overall strategy by the user.

7. CALCULATION OF LIMIT POINT

As indicated previously, the determinant of the tangent stiffness matrix is zero at the limit point and consequently

the system of incremental equations does not possess an unique solution. This can be overcome by constraining the system in some way, such as through enforcement of a prescribed value of a particular displacement. This approach has been adopted in a variety of different forms by many investigators in geometrically nonlinear finite element analysis, e.g., Refs. 19-23. The approach adopted here represents an extension of a scheme described by Zienkiewicz (Ref. 23).

First, a representative degree-of-freedom (Δ_r) is identified. The central displacement of a plate or shell is an appropriate choice, the selection being input directly by the user. A change ($\delta\Delta_r$) in the magnitude of this displacement component is likewise specified. The value of the corresponding change in load intensity ($\delta\eta$) is sought, this being equal to the difference in intensities between the (i)th and (i+1)th load intensities, i.e., $\delta\eta = \eta_{i+1} - \eta_i$. The total incremental loading is given by $\delta\eta\ \{\bar{P}\}$. Three loading and support conditions are analyzed: (see Fig. 12)

(1) No loading except for the force $P_r^{(1)}$ necessary to produce the prescribed value $\delta\Delta_r$. P_r^1 is calculated in the manner of a support reaction in this analysis. The calculated displacements are designated as $\{\Delta^1\}$. (This vector includes the specified value $\delta\Delta_r$).

(2) Application of the normalized load vector $\{\bar{P}\}$ with the ith degree-of-freedom held fixed ($\Delta_i = 0$). Calculate the support reaction $P_r^{(2)}$ in this analysis and the displacements $\{\Delta^2\}$.

(3) The out of balance load vector {f}, calculated on the basis of the displacements at the last load level (n_i) is applied with the degree-of-freedom Δ_i held fixed. Calculate the support reaction $P_r^{(3)}$ in this analysis and the displacements $\{\Delta^3\}$.

In combining these cases it is useful to consider two separate conditions. The first combination considers cases (1) and (2) and excludes the effect of out of balance forces (Case 3). For this circumstance the resulting displacement state is given by the displacements $\{\Delta^1\}$ less the normalized displacements $\frac{1}{P_r^{(2)}}\{\Delta^2\}$ times the force $P_r^{(1)}$, i.e.

$$\{\Delta^1\} - \frac{P_r^{(1)}}{P_r^{(2)}}\{\Delta^2\}$$

This gives the displacement state corresponding to zero reactive force at Δ_r for simple incrementation (no out of balance force correction).

The second combined condition takes into account the influence of the out of balance force correction. By reasoning similar to that given above for the first combined condition, the resulting displacements are

$$\frac{P_r^{(3)}}{P_r^{(1)}}\{\Delta^1\} + \{\Delta^3\}$$

For the modified incremental approach the out of balance loads have to be added over and above the loads of case (2). It is important to keep these load vectors separate during the solution stage because at that point the reactions $P_r^{(1)}$, $P_r^{(2)}$

and $P_r^{(3)}$, and hence the factors of the above combinations, are still unknown.

Unfortunately, the combination of cases (1) and (3) gives no control over the displacement at the degree of freedom Δ_r but in fact defines the value of the load there. In consequence, at the limit point, where $P_r^{(1)}$ becomes zero (this is instantaneously the snapping through circumstance and the specified value $\delta\Delta_r$ is accomplished with theoretically no required force $P_r^{(1)}$), the displacements become infinite. The problem is circumvented by neglecting the out of balance loads in the proximity of the limit point. The criterion used in deciding when to neglect the out of balance loads is the following

$$P_r^{(3)} \geq P_r^{(1)}$$

Thus, in summary, the following combinations of cases are used.

For $P_r^{(3)} < P_r^{(1)}$

$$(1 + \frac{P_r^{(3)}}{P_r^{(1)}}) \{\Delta^1\} - \frac{P_r^{(1)}}{P_r^{(2)}} \{\Delta^2\} + \{\Delta^3\} = \{\delta\Delta\} \qquad (40)$$

where $\{\delta\Delta\}$ is the increment of the total displacement state due to $\delta\Delta_r$, and for $P_r^{(3)} \geq P_r^{(1)}$

$$\{\Delta^1\} - \frac{P_r^{(1)}}{P_r^{(3)}} \{\Delta^2\} = \{\delta\Delta\} \qquad (41)$$

The change in load intensity can be determined after calculation of the increment of displacements as

$$\delta\eta = \frac{p_r^{(1)}}{p_r^{(2)}} \tag{42}$$

or, since

$$\eta_{i+1} = \frac{p_r^{(1)}}{p_2^{(2)}} + \eta_i \tag{43}$$

It should be noted that after the limit point the ratio $p_r^{(1)}/p_r^{(2)}$ becomes negative, thereby reducing the load level until a minimum is reached at a snapback load, after which it increases again.

To apply the prescribed displacements to the linear incremental equations the following approach (Ref. 24) is adopted.

1) The origin of the displacement to be prescribed is changed. Thus, $(\delta\Delta_r + \Delta_r)$ replaces Δ_r. By substitution in the equilibrium equations

$$[K_T]\{\Delta\} = \{P\} - [K_T]\{\bar{\Delta}\} \tag{44}$$

where $\{\bar{\Delta}\}$ consists of zeros everywhere except for freedom r which contains $\delta\Delta_r$. The modification to the load vector $\{P\}$ need only be carried out at freedoms coupled to the constrained freedom.

2) Δ_r is set to zero. This is accomplished by uncoupling the rth equation from the rest, by multiplying the diagonal term by a large number, say 10^{20}.

Finally, after solution of the equations the reaction at freedom r is

$$P_r = -10^{20}\,\Delta_r\,K_{T_r} \tag{45}$$

This procedure is obviously valid if there is more than one prescribed displacement.

8. CALCULATION OF BIFURCATION STATE

a. Linear

The method of calculating the intensity of load (η_c) for bifurcation and the associated mode shape is based on the condition of zero value of the determinant of the tangent stiffness at this point. This condition holds because of the lack of uniqueness of the load displacement path at the bifurcation point, resulting in the singularity of $[K_T]$. The rank of the singularity depends on the number of paths present at the bifurcation point. In this development attention is restricted to cases where only two such paths are present. For these cases the singularity is of rank one.

It should be noted that past reports of this research (Refs. 9 and 10) have emphasized approaches to calculation of bifurcation which depend on the condition stated above. The following description differs from these principally in the computational mechanics.

The problem of linear stability, characterized by a linear pre-buckling state, is examined first. The condition cited above can be written for the general nonlinear representation as

$$|K_T| = |[K_o] + [K_1] + [K_2]| = 0 \qquad (46)$$

where $|\ |$ denotes the determinant of the indicated matrix. To transform this to the linear buckling problem the matrix $[K_2]$ is neglected. This matrix is in fact zero in the absence

of coupling between inplane and out-of-plane displacements on the fundamental path, as in the case of flat plates. Secondly, the $[K_1]$ geometric stiffness matrix is assumed to vary linearly with the load level η. This assumption is justified if the distribution of internal forces in the structure does not change along the fundamental path.

The problem therefore becomes one of finding the critical load level (η_c) such that

$$|[K_o] + \eta_c [K_1(\bar{\Delta})]| = 0 \tag{47}$$

where $\{\bar{\Delta}\}$ are the displacements corresponding to a normalized load vector ($\eta = 1$).

The determinant expressed in Eq. (47) is first established at two points, $\eta = 0$ and $\eta = 1$. These two points furnish sufficient information for starting a Lagrangian interpolative scheme which subsequently progresses in an iterative fashion. An analytical expression of polynomial form is sought for η in terms of already-calculated values of load intensity (η_j) and the determinants (Det.j) expressed by Eq. (47) at these intensities. This form is obtained by Lagrangian interpolation and writing the result as an equation which gives the intensity (η_{i+1}) for a zero value of the corresponding determinant one has

$$\eta_{i+1} = \sum_{j=1}^{i} \eta_j \left(\prod_{k=1}^{i(k\neq j)} \frac{\text{Det. } k}{\text{Det.k-Det.j}} \right) \tag{48}$$

The process is shown schematically in Fig. 12. Each iteration

consists of the following steps

1) Scale element geometric stiffnesses $[K_1]$ by η_{i+1} and add into total stiffness matrix which is initialized to $[K_0]$.
2) Decompose total stiffness matrix into upper triangular form by Gaussian Elimination procedure.
3) Evaluate determinant by multiplying the diagonal terms.
4) Perform Lagrangian interpolation to obtain a better estimate of the load required to yield zero determinant.

The iteration procedure continues until two successive values of η are within a predefined tolerance.

After convergence of the above procedure, the eigenvector can be calculated with very little extra computational effort. The problem formulation is now that of finding a displacement vector $\{\Delta\}$ that satisfies the following relationship.

$$[K_o + \eta_c K_1(\bar{\Delta})]\{\Delta\} = 0 \qquad (49)$$

The decomposition of these equations into upper triangular form has already been performed during the last iteration of the eigenvalue procedure. To insure a nontrivial solution for $\{\Delta\}$, before proceeding with the backsubstitution, the right hand side is initialized to zero except for the last entry which is given a value of unity, as is the last diagonal term of the decomposed matrix. By this artifice the last displacement in the structure is forced to take a value of unity, and thus the eigenvector is normalized with respect to this displacement. Note that this method will yield a

nontrivial eigenvector flat plates and beams, only if the last freedom in the structure is a bending displacement. The user must ensure this by the way he numbers the nodal points in the idealization.

The choice of the last equation for discarding is rather arbitrary. In the present case the choice is dictated by computational simplicity. Wilkinson (Ref. 25) has shown that for some matrices inaccurate results are obtained unless one particular equation is discarded. Because of this he suggests a symmetric strategy: inverse iteration. In this method an approximate eigenvector $\{\Delta_i\}$ yields an improved approximation $\{\Delta_{i+1}\}$ by the following procedure.

$$[K_o + \eta_c K_1(\bar{\Delta})] \{\Delta_{i+1}\} = \{\Delta_i\} \tag{50}$$

As already noted, the matrix on the left hand side of Eq. (50) has been triangularized during the last iteration of the eigenvalue procedure. Thus, successive resolutions of the equations indicated by Eq. (50) are called for with the right hand side consisting of the displacement vector from the last iteration. This procedure is computationally quite inexpensive because the elimination procedure has to be performed only on the right hand side. This algorithm has been found (Ref. 26) to converge in a few cycles in most cases.

In the present study the eigenvector obtained by discarding the last equation has proven to be highly accurate. If the accuracy of this solution proves to be suspect for a class of problems not yet solved the inverse iteration scheme described above can be incorporated with a minimal effort.

b. Nonlinear

The approach of the last section, wherein the determinant of the tangent stiffness matrix $[K_T]$ is equated to zero, is again used as the basis for predicting nonlinear buckling. In the presence of nonlinearities in behavior along the fundamental path the simplifying assumptions exploited to simplify the problem to a linear one are no longer valid. In other words, $[K_2]$ is retained, and $[K_1]$ is not assumed to be linearly dependent on η. Consequently, the nonlinear buckling problem is far more complex to solve than its linear counterpart.

In the present study, the load-deflection curve of the structure is followed up to bifurcation. An incremental procedure is used for this, so that the determinant of the tangent stiffness matrix can be monitored during the analysis. Constant load increments are used throughout, so that Lagrangian interpolation with equal intervals is used to predict where the determinant goes to zero. A comparison of linear and nonlinear buckling with respect to the determinant-load level plot, is shown in Figure 12. When the load level has reached a point such that buckling will occur during the next load increment a linear buckling analysis is performed. The last tangent stiffness matrix calculated takes the place of the linear stiffness matrix in Equation (49).

9. NUMERICAL ANALYSES

Numerical solutions to four nonlinear problems are described in this section. These have been chosen because of the availability of comparison solutions.

The first problem is the case of a constant thickness (t) isotropic square plate subjected to uniform uniaxial compression (see inset, Fig. 13). The boundary conditions of the finite element analyses consist of simple support with respect to flexure (i.e., zero normal displacement and normal bending moment along the edges) and complete freedom for the edges to displace in the plane of the plate. Initial imperfections are present as represented by a normal displacement of the middle surface, distributed in double sinusoidal form, with a central amplitude 0.1t. Because of the symmetry of load, geometry and structural response the analyses are performed for only a quadrant of the plate.

The solutions of the problem are presented in Fig. 13 in the form of a plot of the ratio of total applied load (P) and the critical load for linear stability (P_{cr}) versus the ratio of the central deflection (w) and the plate thickness. It is seen that the range of solutions extends to $P/P_{cr} = 2$.

A classical solution for this problem due to Coan (Ref. 27) is presented along with the finite element solutions, that are in each case based upon load increments of $P_{cr}/10$. It is appropriate to first consider the results obtained by use of a full Newton-Raphson iterative scheme, in which iterations in each load increment are continued until convergence

is achieved. These are given for idealizations consisting of two elements (the 1 x 1 grid in the quadrant, consisting of 2 triangles) and 8 elements (the 2 x 2 grid). It is seen that these converge to a solution to the right of the classical solution, i.e., a solution that is less stiff than the classical solution. The modified incremental approach (the tangent stiffness procedure combined with a one-step Newton-Raphson correction) is applied to the 8-element representation. It is interesting to note that for the chosen load increment the difference between the full Newton-Raphson and the less expensive modified incremental results is negligible.

The discrepancy between the classical solution and the above finite element solutions is due in part to the constraint of the former to linear inplane displacement of the loaded edges. This gives a stiffening effect. It is not customary in finite element analysis to enforce such an idealized state upon the edge conditions and in the above-described finite element solutions the inplane edge displacements were not constrained to give a linear variation. When this constraint is enforced for a 2-element (1 x 1 mesh) finite element solution, stiffer results than Coan's are obtained (see values denoted by x in Fig. 13), as expected.

The second nonlinear analysis problem is shown in Figure 14. A cylindrical segment is fixed along all sides and is subjected to pressure loading. The solutions to be discussed involve the calculation of the central deflection (w_c) as a function of the applied pressure. Brebbia and Connor (Ref. 28)

first solved this problem with use of rectangular shell elements based on assumed displacements, i.e., a stiffness formulation. Lien (Ref. 29) also employed rectangular shell elements. Prato (Ref. 30) applied a mixed, Reissner-type shell element to this problem. Dhatt (Ref. 31) utilized a discrete-Kirchoff approach. Finally, it should be noted that Connor and Morin (Ref. 32) have reported numerical results for this problem.

Results from the present formulation, for a 3 x 3 (18-element) gridwork, are shown in Fig. 14. Advantage is taken of symmetry, with a 3 x 3 (18-element) gridwork in a quadrant of the shell. None of the alternative numerical solutions from Refs. 28-32 gives tabulated data and it is felt that the graphical representations in these references, except for Ref. 31, cannot be transcribed with the accuracy associated with plotted comparisons.

The basic difference in these results, up to a pressure of approximately 0.150 is accounted for by the difference in linear solutions, the Ref. 31 results being based on a different variational principle with 9-term expansions for u, v, and w and independent quadratic expansions for the middle surface slopes. These same considerations may have influence on the nonlinear solutions. Although, as noted above, Ref. 32 does not give data that is accurate enough for plotted comparisons, it appears to the authors to have a solution that corresponds more closely to the present work.

The third nonlinear analysis problem pertains to the spherical cap shown in Fig. 15, which is subjected to a concentrated load P at the crown. The support conditions involve the restraining of displacements normal to the edge and normal to

the shell itself. Thus translations along the edge of the shell is permitted. This type of support condition is sometimes described as 'hinged'.

This structure exhibits a snap-through behavior under the indicated load with eventual recovery of stiffness at higher displacements. A classical (series) solution for the problem has been obtained by Leicester (Ref. 33) and an alternative finite element solution by Dhatt (Ref. 31) who, as was noted previously adopts a discrete-Kirchoff approach.

Again, a 3 x 3 grid (18-elements) is employed within a quadrant of the structure. Results are shown in Fig. 15 for the central deflection as a function of the applied load. The agreement among the three solutions is remarkably good through two limit points, up to where a stiffening behavior is again experienced. As is usual with the incremental approach the displacements tend to lag behind the true solution for increasing loads. Despite this, the value of the snap-through load is predicted very accurately by the present method.

To verify the accuracy of the quadrilateral element formulation the problem of a square clamped plate under pressure loading is considered. A 4 x 4 idealization is used for one quarter of the plate as shown in Fig. 16. The analysis proceeds to a load level that produces considerable nonlinear behavior. The modified incremental approach is used to solve the nonlinear equations. The results are displayed in Fig. 16 along with the classical solution of Levy (Ref. 35), and other finite element solutions. Again the present results lag slightly behind the true solution.

10. CONCLUDING REMARKS

This report has presented the formulation, for geometrically nonlinear analysis, of a curved triangular thin shell finite element together with computational approaches which enable the use of the element formulation in a variety of thin shell instability calculations. The linear aspects of the element formulation are described in a separate report (Ref. 1). The types of instability calculations which were effected included bifurcation and limit point analyses.

The basis of the finite element formulation was a cubic polynomial field within the element. Although this is close to the simplest formulation that can be attempted for triangular elements which evidence bending, it is not efficient when used without modification due to the discontinuity of normal slope across element interfaces. The requirement of slope continuity is therefore written as a constraint condition and is appended to the global equations by means of the Lagrange multiplier technique. Numerical analyses presented in this report and in Ref. 1 show that efficient solutions are obtained in this manner for an extensive range of comparison problems. Displacement fields which were simpler than those used in the linear formulation were used in the development of terms for geometrically nonlinear behavior. This approach, known as an "inconsistent" formulation, did not significantly prejudice the accuracy of the problems solved numerically.

The cornerstone of all of the types of nonlinear analyses presented herein was the modified incremental method, which combines a conventional incremental, or tangent, step with a

one-cycle Newton-Raphson calculation. Numerical comparisons showed that the adopted approach strikes a balance between accuracy and computational efficiency for the problems solved. An alternative approach was presented for the solution of the nonlinear algebraic equations, based upon treatment of these equations as an initial value problem. This approach was demonstrated for a simple test problem but was not applied to the large-scale numerical analyses. It features the rational selection of step size and the attainment of solution accuracy within prescribed limits and therefore appears worthy of further study and improvement.

REFERENCES

1. Thomas, G. R. and Gallagher, R. H., A Triangular Thin Shell Finite Element: Linear Analysis, NASA CR-2483, 1975.

2. Martin, H. C., "Finite Element Formulation of Geometrically Nonlinear Problems". Recent Advances in Matrix Methods of Struct. Analysis and Design. R. H. Gallagher, et al, Ed., Univ. of Alabama Press, 1971, pp. 343-381.

3. Oden, J. T., "Finite Element Applications in Nonlinear Structural Analysis", Proc. of Symp. on Application of Finite Element Methods in Civil Engrg, W. Rowand and R. Hackett, Eds., Vanderbilt Univ., Nashville, Tenn., 1969, pp. 419-456.

4. Stricklin, J., Haisler, W. and Von Riesemann, W., "Evaluation of Solution Procedures for Material and/or Geometrically Nonlinear Structural Analysis", AIAA J., V. 11, No. 3, 1973, pp. 292-299.

5. Gallagher, R. H., "Geometrically Nonlinear Finite Element Analysis", Proc. of Specialty Conf. on the Finite Element Method in Civil Engrg., McGill Univ., June 1972.

6. Yamada, Y., "Incremental Formulation for Problems with Geometric and Material Nonlinearities", Advances in Computational Methods in Struct. Mech. and Design, J. T. Oden, et al, Ed., Univ. of Alabama Press, 1972, pp. 325-356.

7. Koiter, W., "A Consistent First Approximation in the General Theory of Thin Elastic Shells", in The Theory of Thin Elastic Shells, W. Koiter, Ed., North-Holland Publ. Co., Amsterdam, 1960, pp. 12-33.

8. Harvey, J. and Kelsey, S., "Triangular Plate Bending Element with Enforced Compatibility", AIAA J., V. 9, No. 6, 1971, pp. 1023-1026.

9. Mau, S. T. and Gallagher, R. H., A Finite Element Procedure for Nonlinear Pre-Buckling and Post-Buckling Analysis, NASA CR-1936, January 1972.

10. Mau, S. T. and Gallagher, R. H., A Method of Limit Point Calculation in Finite Element Structural Analysis, NASA CR-2115, Sept. 1972.

11. Mushtari, K. and Galimov, K., Nonlinear Theory of Elastic Shells, NASA TT-F62, 1962.

12. Thomas, G. R., Finite Element Nonlinear Analysis of Shells. Ph.D. Dissertation, Cornell University, Aug. 1973.

13. Rajasekaran, S. and Murray, D., "On Incremental Finite Element Matrices", Proc. ASCE, J. of the Struct. Div. V. 99, No. ST 12, 1973, pp. 2423-2438.

14. Mallett, R. and Marcal, P. V., "Finite Element Analysis of Nonlinear Structures", Proc. ASCE, J. of the Struct. Div., V. 94, No. ST9, 1968, pp. 2081-2105.

15. Thurston, G., "Continuation of Newton's Method Through Bifurcation Points", J. of Applied Mech., V. 36, No. 3, 1969, pp. 425-430.

16. Bulirsch, R. and Stoer, S., "Numerical Treatment of Ordinary Differential Equations by Extrapolation Methods", Num. Math, V. 8, p. 1-13, 93-104, 1966.

17. Acton, F. S., Numerical Methods that Work. Harper and Row, New York, 1970. pp. 805-823.

18. Stricklin, J. A., Naisler, W. E. and Von Riesemann, W. A., "Geometrically Nonlinear Structural Analysis by Direct Stiffness Method". Proc. ASCE, J. of the Struct. Div., V. 97, No. ST9, 1971, pp. 2299-2314.

19. Pian, T. H. H. and Tong, Pin, "Variational Formulation of Finite Displacement Analysis", Proc. of IUTAM Symp. on High Speed Computing of Elastic Structures, Tome 1, Univ. of Liege Press, 1971, pp. 43-64.

20. Roberts, T. M. and Ashwell, D. G., "The Use of Finite Element Mid-Increment Stiffness Matrices in the Post-Buckling Analysis of Imperfect Structures", Int. J. Solids Struct., V. 7, 1971, pp. 805-823.

21. Sharifi, P. and Popov, E., "Nonlinear Buckling Analysis of Sandwich Arches", Proc. ASCE, J. of the Engrg. Mech. Div., V. 97, No. EM5, 1971, pp. 1397-1412.

22. Wright, E. W. and Gaylord, E. H., "Analysis of Unbraced Multistory Steel Rigid Frames", Proc. ASCE, J. of the Struct. Div., No. ST5, 1968, pp.

23. Zienkiewicz, O. C., "Incremental Displacement in Non-Linear Analysis", Int. J. Num. Meth. in Engrg., V. 3, 1971, pp. 587-588.

24. Irons, B., "A Frontal Solution Program for Finite Element Analysis", Int. J. Num. Meth. in Engrg., V. 2, 1970, pp. 5-32.

25. Wilkinson, J. H., The Algebraic Eigenvalue Problem, Oxford U. Press, London, 1965.

26. Clough, R. W. and Bathe, K. J., "Finite Element Analysis of Dynamic Response", Advances in Computational Methods in Structural Mechanics and Design. Oden, J. T., et al, Editors. Univ. of Alabama Press, 1972, pp. 153-179.

27. Coan, J. M., "Large Deflection Theory for Plates with Small Initial Curvature Loaded in Edge Compression", Trans. ASME, J. of Appl. Mech., V. 18, 1951.

28. Brebbia, C. and Connor, J., "Analysis of Geometrically Nonlinear Plates and Shells by the Finite Element Method", Proc. ASCE, J. of the Engrg. Mech. Div., V. 95, No. EM2, 1969, pp. 463-483.

29. Lien, S., Finite Element Elastic Thin Shell Pre- and Post-Buckling Analysis, Ph.D. Thesis, Cornell University, 1971.

30. Prato, C., A Mixed Finite Element for Thin Shell Analysis Ph.D. Thesis, Dept. of Civil Engrg., Massachusetts Inst. of Technology, May 1968.

31. Dhatt, G. S., "Instability of Thin Shells by the Finite Element Method", Proc. IASS Symposium for Folded Plates and Prismatic Structures, Vienna, 1970.

32. Connor, J. J. and Morin, N., "Perturbation Techniques in the Analysis of Geometrically Nonlinear Shells", Proc. of IUTAM Symp. on High Speed Computing of Elastic Structures, Tome 2, Univ. of Liege Press, 1971, pp. 683-705.

33. Leicester, R. H., "Finite Deformations of Shallow Shells" Proc. ASCE, J. of the Engrg. Mech. Div., No. EM6, V. 94, 1968, pp. 1409-1421.

34. Anderheggen, E., "A Conforming Triangular Finite Element Plate Bending Solution", Int. J. Num. Methods Engrg., Vol. 2, pp. 259-264, 1970.

35. Levy, S., "Square Plate with Clamped Edges Under Normal Pressure Producing Large Deflections", NACA TN-847, 1942.

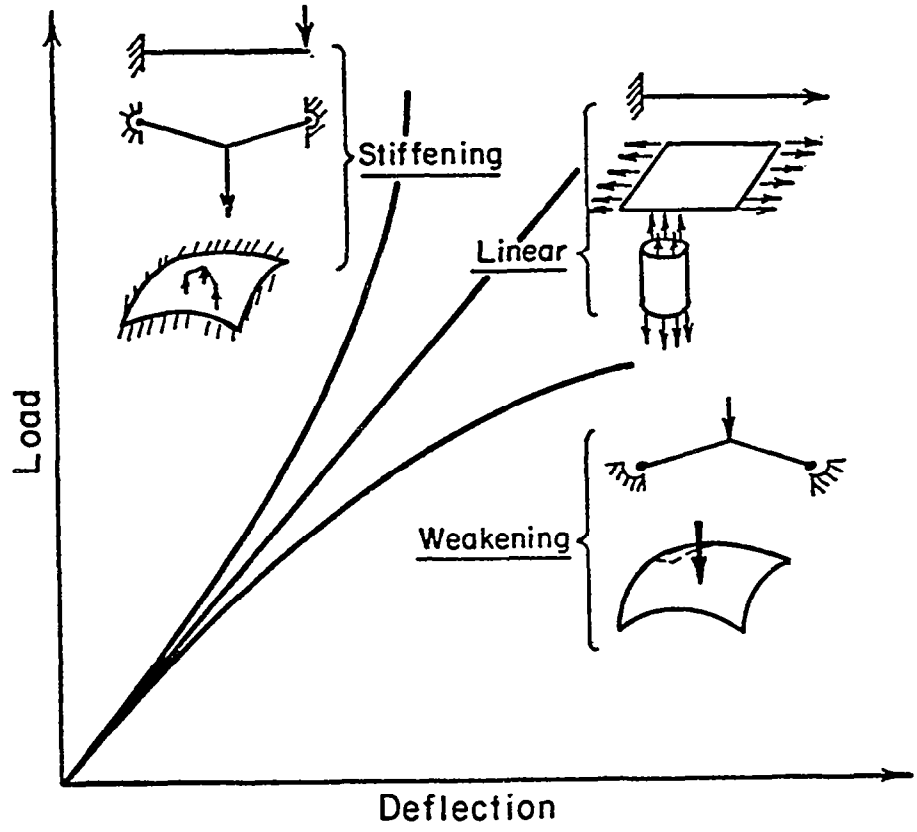

Figure 1. Forms of Nonlinear Force-Displacement Response

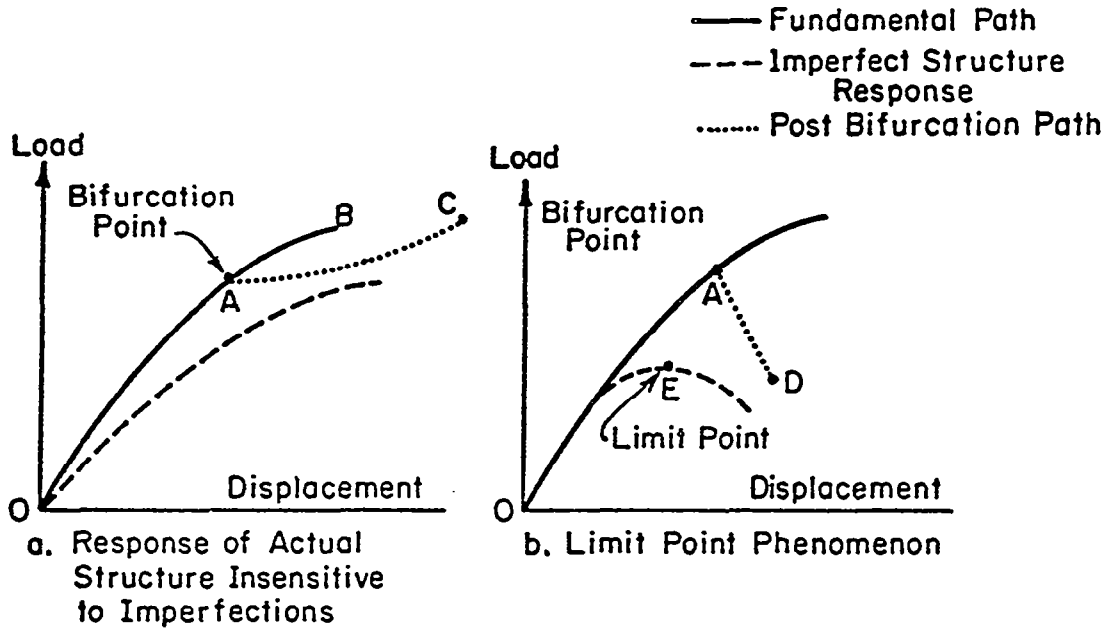

Figure 2. Critical Load Phenomena

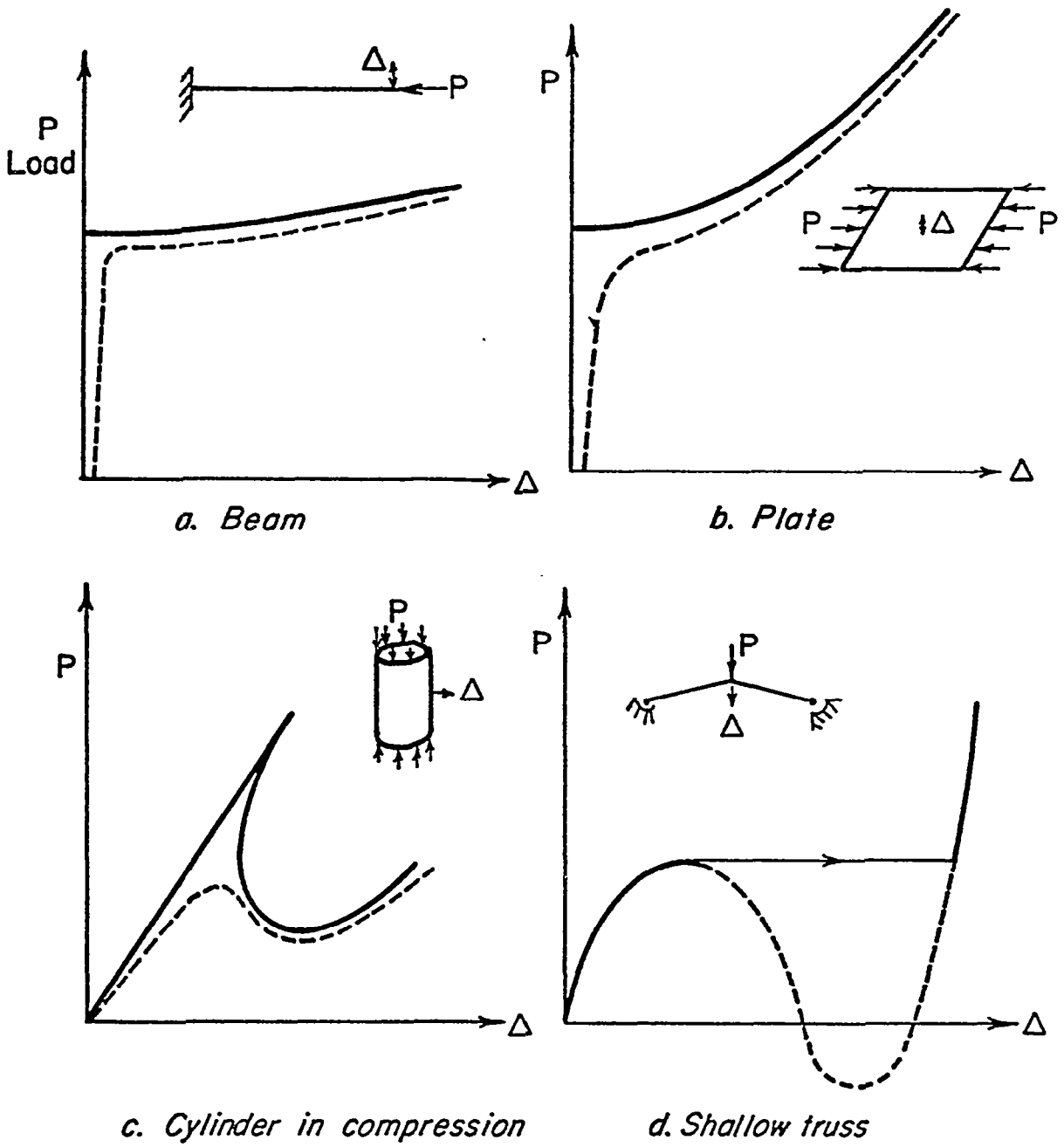

Figure 3. Examples of Structures Sustaining Various Forms of Instability and Nonlinear Force-Displacement

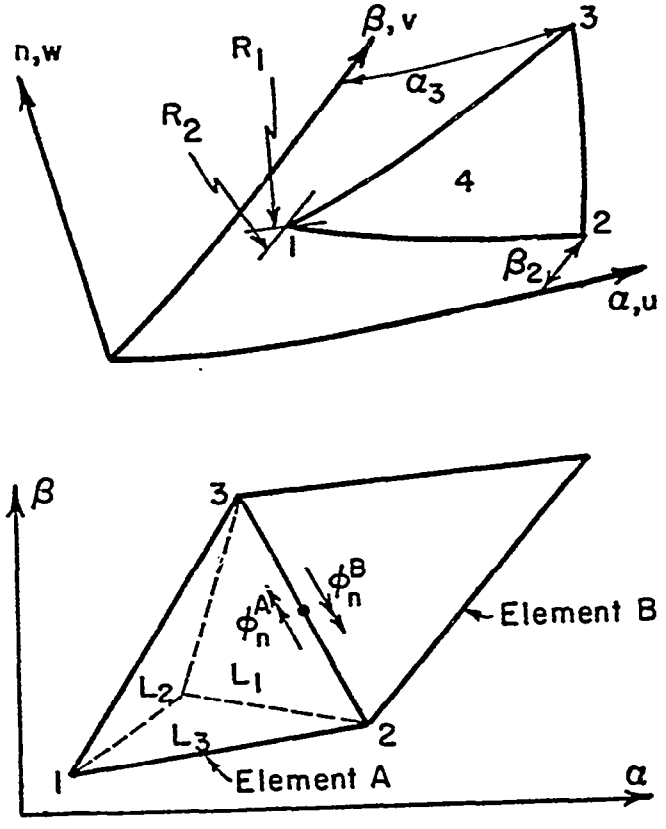

Figure 4. Triangular Thin Shell Element

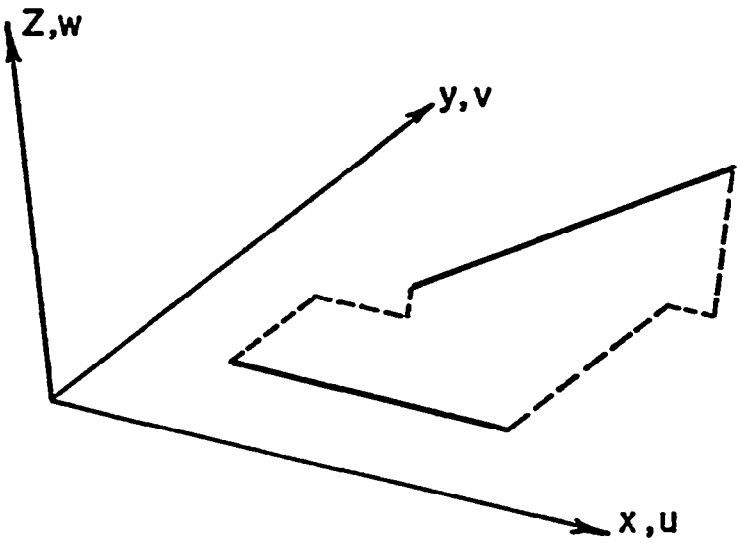

Figure 5. Axial Member-Geometrically Nonlinear Behavior

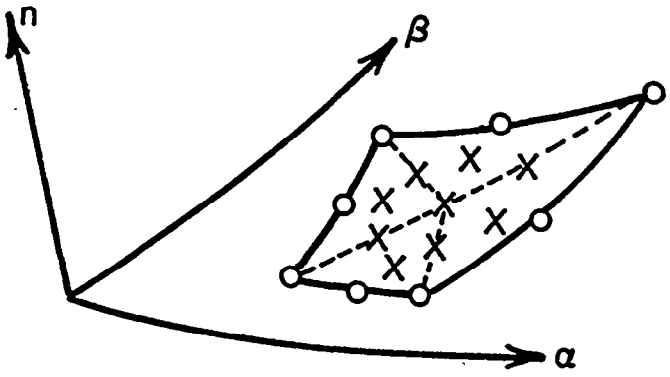

O Retained nodal point

X Eliminated nodal point

Figure 6. Quadrilateral for Inconsistent Formulation of Nonlinear Matrices

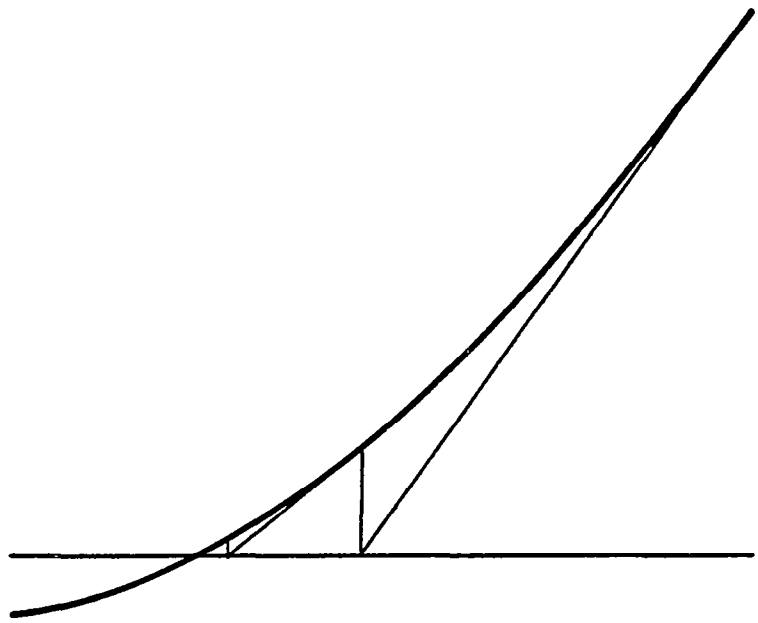

a. Newton's method

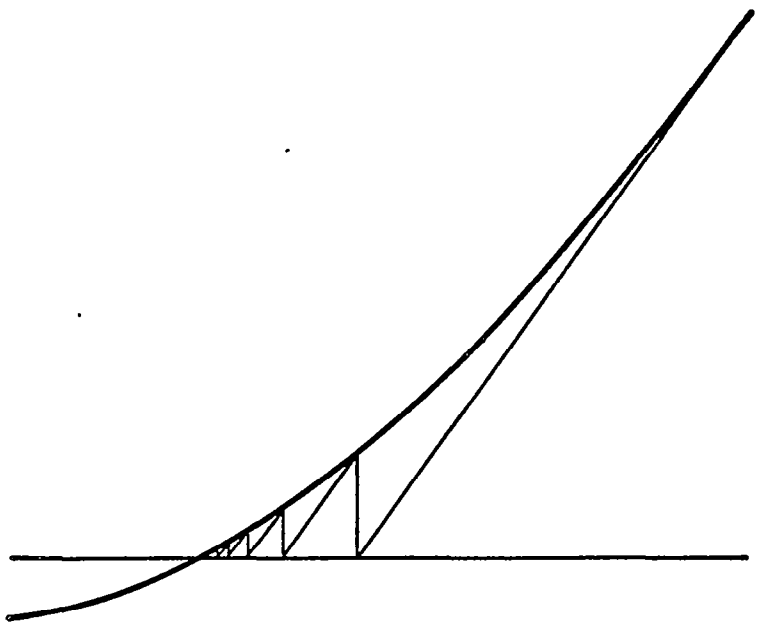

b. Modified Newton

Figure 7. Newton-Raphson Iteration

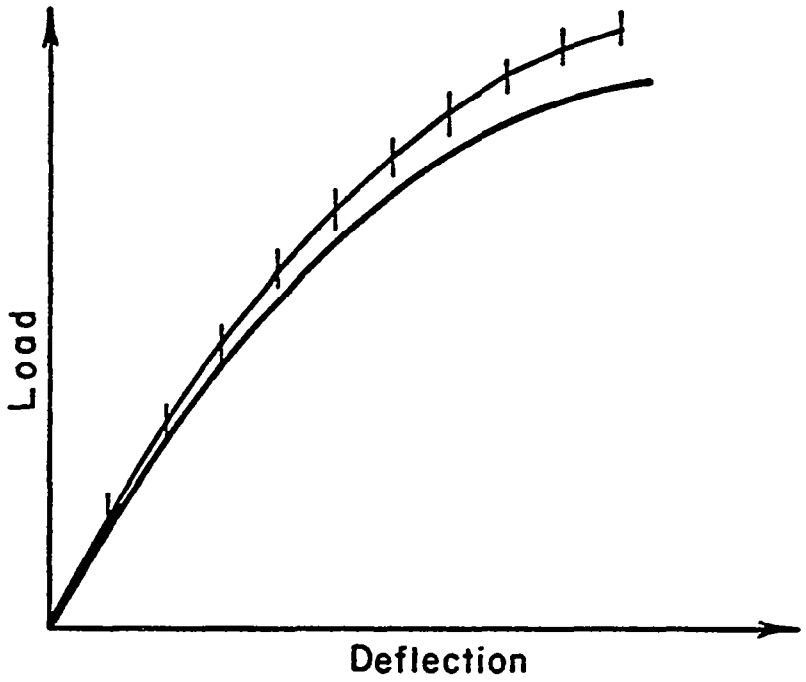

Figure 8. Incremental Analysis

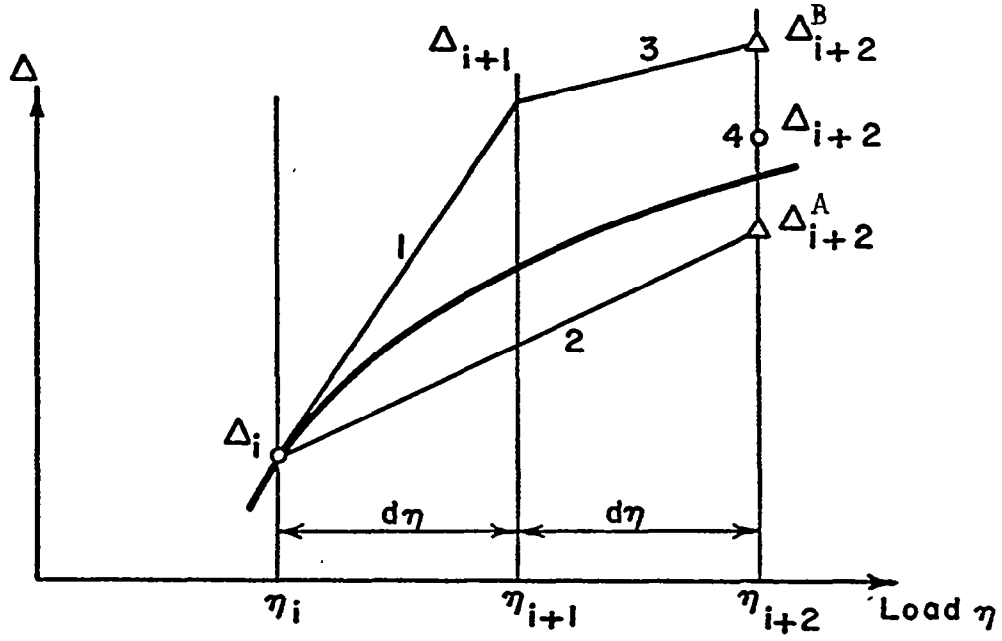

Figure 9. Error Estimation by Use of the Bulirsch and Stoer Method

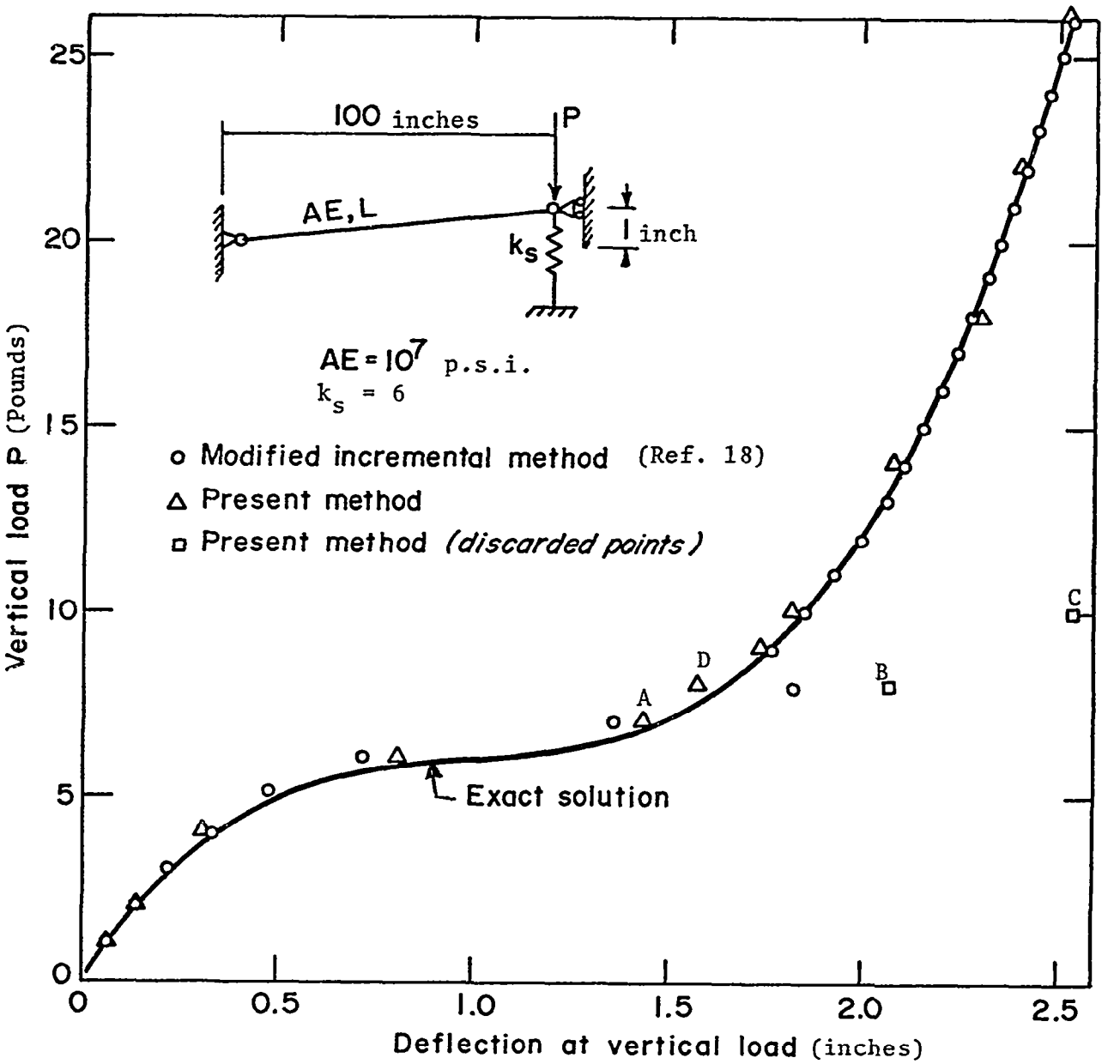

Figure 10. Solution Comparisons-Shallow Truss Problem

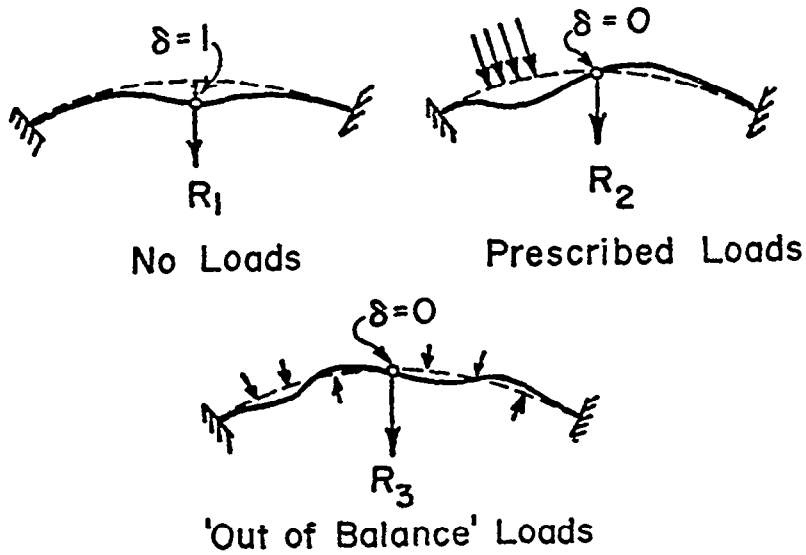

Figure 11. Method of Limit Point Calculation

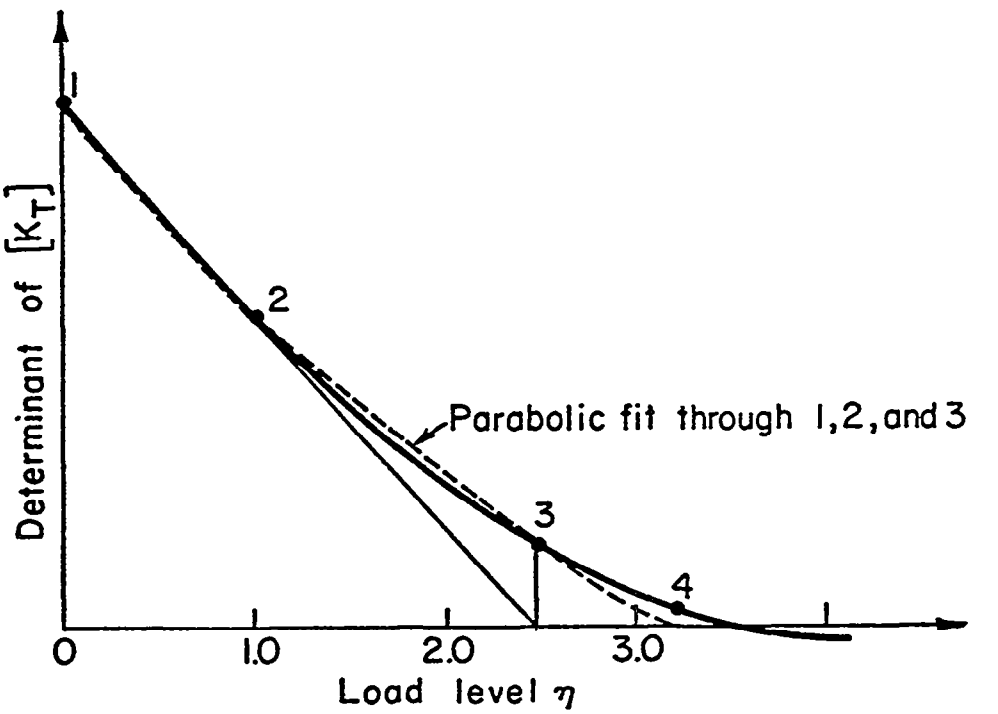

a. Linear buckling analysis

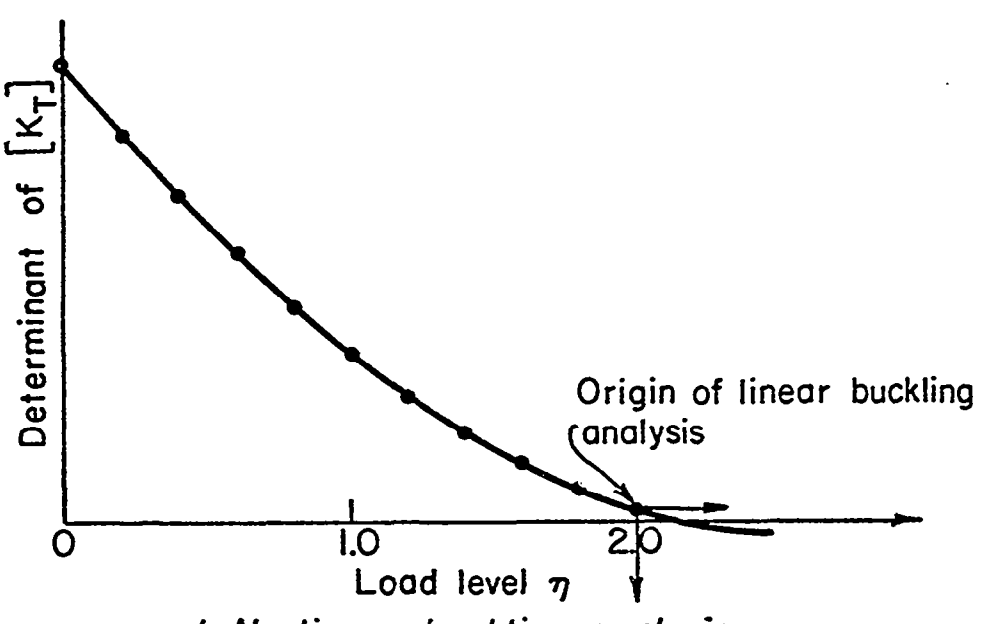

b. Nonlinear buckling analysis

Figure 12. Calculation of Bifurcation Load

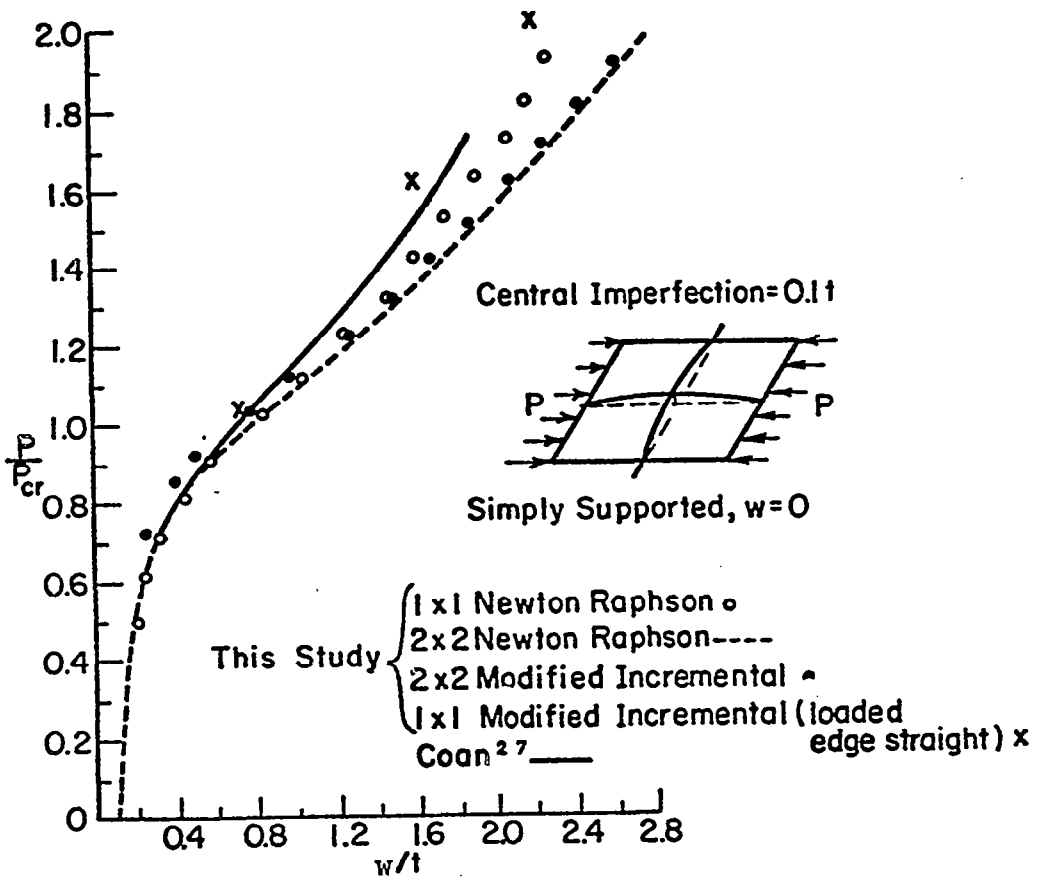

Figure 13. Imperfect Plate Under Edge Compression

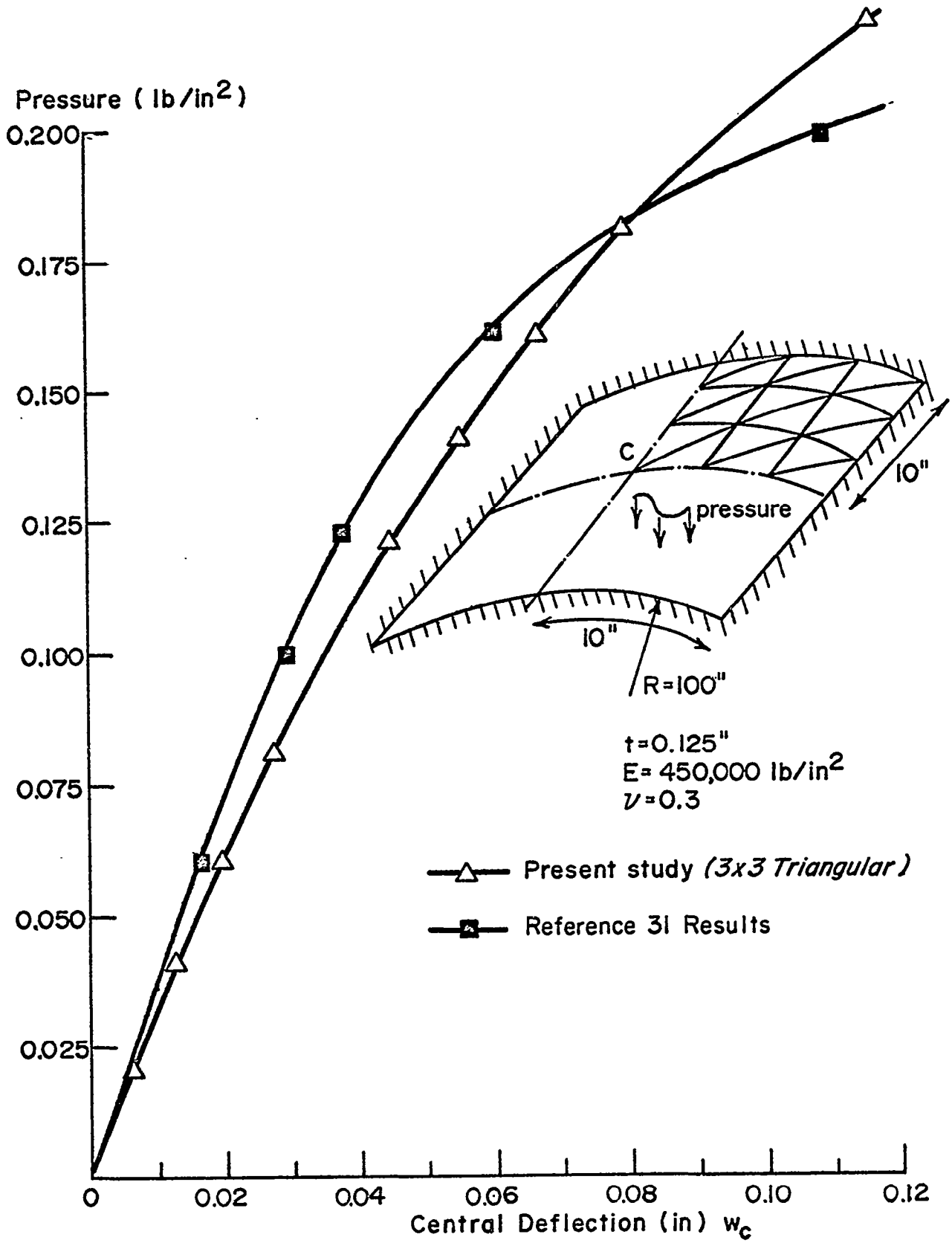

FIGURE 14. PRESSURE-LOADED CYLINDRICAL SHELL SEGMENT

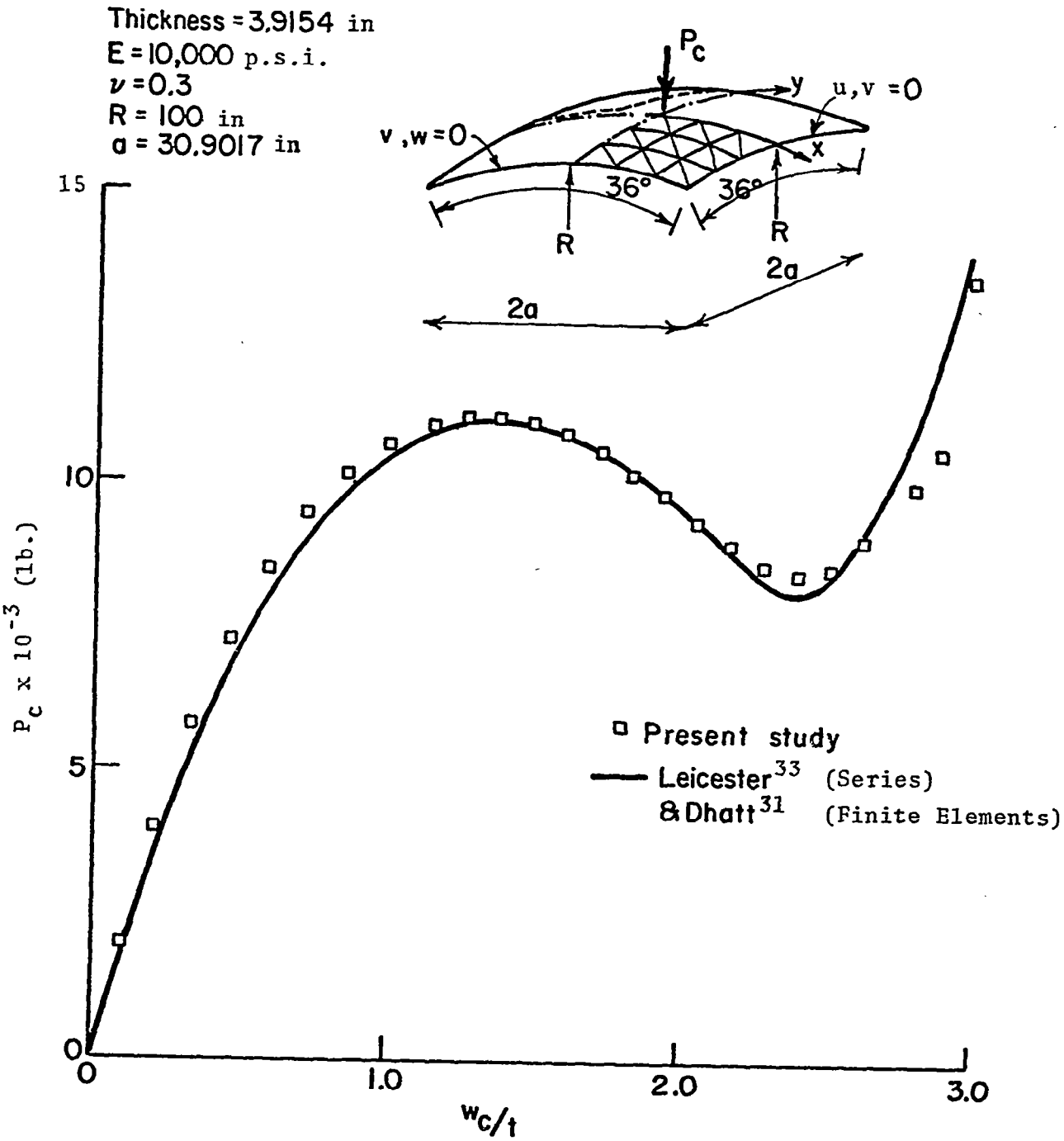

Figure 15. Spherical Cap Under Concentrated Load at Crown

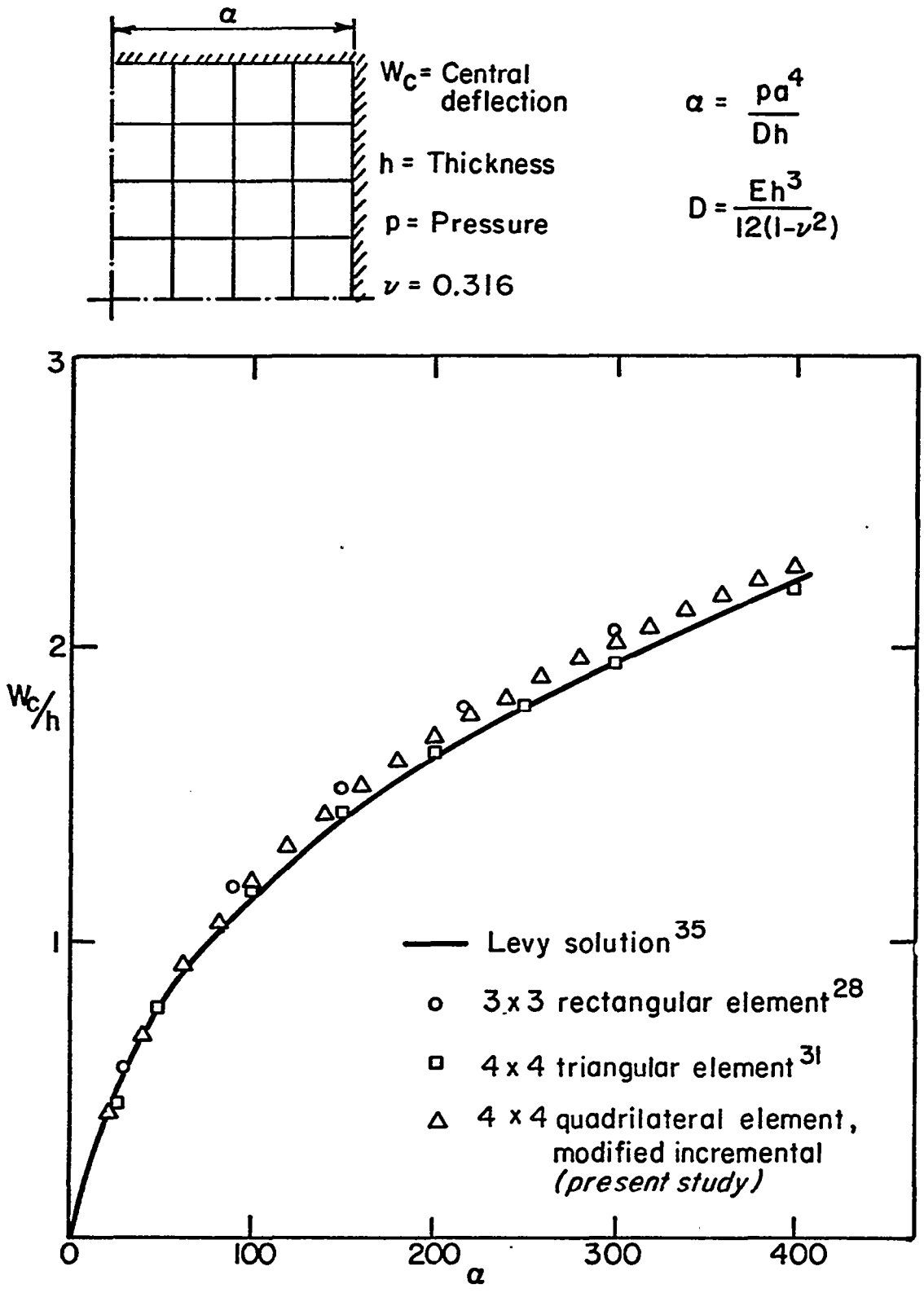

Figure 16. Clamped Square Plate Under Pressure Load